1965

On the rate of crack extension due to transverse shear fatique loading

William J. Valentine
Lehigh University

ON THE RATE OF CRACK EXTENSION

DUE TO TRANSVERSE SHEAR FATIGUE LOADING

by

William J. Valentine

A Thesis

Presented to the Graduate Faculty

Of Lehigh University

in Candidacy for the Degree of

Master of Science

Lehigh University

1965

This thesis is accepted and approved in partial fulfillment of the requirements for the degree of Master of Science.

9/20/65
(date)

Fazil Erdoğan
Professor in charge

Ralph H. Long Jr.
Head of the Department

Acknowledgement

I wish to express my special appreciation to Dr. Fazil Erdogán for the assistance and suggestions he provided and for his help in the preparation of this paper. I also wish to thank Professor T.E. Jackson for his advice in the design and construction of the machine and Dr. Roberts for his guidance throughout the project and his suggestions for the preparation of the report. Part of the expense for the construction of the machine has been provided by a grant from the National Aeronautics and Space Administration (NGR 39-007-011).

Table of Contents

NOMENCLATURE

$2a$	horizontal crack length
h	thickness of the plate
k_1	symmetric component of the stress-intensity factor for extension
k_2	skew-symmetric component of the stress-intensity factor for extension
N	number of cycles
Q	maximum transverse shear loading
r	distance from the crack tip to the stressed element
K_1	symmetric component of the stress-intensity factor for bending
K_2	skew-symmetric component of the stress-intensity factor for bending
θ	the angle from the horizontal to the stressed element
δ	the distance from the neutral plane of the plate
r,θ	polar coordinate system
$\sigma_r, \sigma_\theta, \tau_{r\theta}$	stress components in a polar coordinate system
σ_o	stress due to tensile loading
σ_b^∞	surface stress due to symmetric bending moment at infinity
$\frac{da}{dN}$	rate of crack growth
A, B, α_1, γ_2	positive constants
n	speed of revolution of the eccentric in radians per second
K_{cr}	critical stress intensity factor
ϕ	the fraction of the total number of dislocations effectively contributing to the extension of the crack

m	the total number of moving dislocations which contribute to crack extension
b	the magnitude of Burgers vector
p	plastic zone size
p_e	plastic zone size due to plane extension
p_b	the range of the plastic zone size due to bending
p_{bs}	plastic zone size due to bending symmetric bending
σ_y	the yield strength of the material

List of Figures

List of Tables

ON THE RATE OF CRACK EXTENSION DUE TO TRANSVERSE SHEAR FATIGUE LOADING

by

William J. Valentine

Abstract

The increasing use of stressed skin construction has given rise to much interest in the study of fatigue crack extension of all types. This thesis is concerned with the design and construction of a machine for the study of crack growth rate phenomena in thin aluminum plates that are subjected to transverse shear loads.

The report includes a theoretical discussion of the transverse shear mode of crack extension, an explanation of the design of the machine, an outline on the testing procedure used, and the results of some preliminary tests.

This report is to serve principally as a guide for future theoretical and experimental studies in this area.

I. Introduction

The fatigue life of any structure may be divided into three distinct subdivisions:[1] crack initiation, crack growth, and total failure. During the period of crack initiation, extremely small microcracks form. After sufficient cyclic loading has taken place, these microcracks coalesce to form a large visible crack, and the period of crack growth begins. In this phase of fatigue life the crack is assumed to grow in a continuous, or at least a quasi-continuous fashion. The total failure of the structure, which occurs during one load cycle, is marked by the occurrence of very rapid crack growth.

In three dimensional structures most of the fatigue life is spent in the crack initiation phase. The period of crack growth is quite small,[2] and total failure will ensue in a few cycles. Since the use of stressed skin construction has become important, increasing interest has arisen in the two dimensional structures such as thin plates and shells. These structures have relatively short crack initiation periods, thus, a majority of their fatigue life is spent in the crack growth phase. In order to better utilize the structures during this period a thorough understanding of crack growth phenomena is required. For this reason a vast amount of qualitative work has been done, and some good quantitative results have even been found. Most of the work has been done in the area of plane extension, which is concerned with the effects of meridional loading on crack propagation. Considerable work has also been done by Roberts[3] on the effects of reversed cyclic bending. One of the important modes of fatigue crack growth, the transverse shear mode, which occurs in cracks near rivets

in aircraft and in cracks in shells with transverse stiffeners has received little attention theoretically or experimentally.

The principal objective of this thesis is, therefore, the design of a simple machine that may be used in the study of growth phenomena of a small crack in an aluminum plate due to a transverse shear fatigue load. The results of some preliminary tests are also included, and an attempt to formulate a qualitative approach to this mode of fatigue growth is presented.

II. Theoretical Considerations

The theoretical model of the transverse shear mode of crack extension is shown in Figure 1. This model, which is based on the assumption that the shear forces are applied at the edge of a crack located in a thin infinite plate, has received some consideration by F. Erdogán and G. Sih [4] in their static analysis of stress intensity factors. The model as presented does not actually propagate the crack by a shear mode as its name implies. When looked at from a mathematical viewpoint, it can be seen to be a bending mode. It is "the tearing mode which is assumed to occur in the skew-symmetric bending of cracked plates or skew-symmetric loading of cracked plates by forces perpendicular to their planes where the displacement discontinuity is perpendicular to the plane of the material and in the plane of the crack." [3] Figure 2 gives some physical insight into the actual mechanism of the crack extension. It can be seen that as the crack is spread in its plane, the crack tip is caused to move by a bending phenomena even though the displacement of the crack edge on itself is caused by a "transverse shear force Q." It is also noted that theoretically the crack edges do not interfere with each other.

If the loading situation depicted in Figure 1 is considered, the equations of stress near the crack tip are: [5]

$$\sigma_r = \frac{\delta 2}{h\sqrt{2r}} \cos\frac{\theta}{2}\left[K_1\left(1 + \sin^2\frac{\theta}{2}\right) + \frac{3}{2}K_2 \sin\theta\right]$$

$$\sigma_\theta = \frac{\delta 2}{h\sqrt{2r}} \cos\frac{\theta}{2}\left[K_1 \cos^2\frac{\theta}{2} - \frac{3}{2}K_2 \sin\theta\right] \qquad (1)$$

$$\tau_{r\theta} = \frac{\delta 2}{h\sqrt{2r}} \cos\frac{\theta}{2}\left[K_1 \sin\theta + K_2(3\cos\theta - 1)\right]$$

where the coordinates of the crack tip are as shown in Figure 3. The values of K_1 and K_2, the stress intensity factors for bending, are functions of the applied external loading and the crack geometry. For the transverse shear loading situation under consideration, K_1 is zero and [6]

$$K_2 = \frac{6Q\sqrt{a}}{\pi h^2} \quad . \tag{2}$$

The direction of crack propagation in any element is known to be perpendicular to the maximum tensile stress at that point. It can be shown that if only this shear loading were used, the crack would grow away from the horizontal initiating crack in the direction $\pm 70.5^{\circ}$ [4] as shown in Figure 4. This would require the solution for a branched crack and make the accurate meaningful measurements of the crack growth a difficult problem. The obvious solution to this problem is the addition of a tensile stress field perpendicular to the initiating crack, (see Figure 5). This stress will not only cause the crack to grow in the desired direction, but also decrease the interference of the crack on itself.

The stresses due to bending near the crack tip will, therefore, have the following stresses due to plain extension superimposed on them: [4]

$$\sigma_r = \frac{1}{\sqrt{2r}} \cos\frac{\theta}{2}\left[k_1\left(1 + \sin^2\frac{\theta}{2}\right) + \frac{3}{2}k_2 \sin\theta\right]$$

$$\sigma_\theta = \frac{1}{\sqrt{2r}} \cos\frac{\theta}{2}\left[k_1\cos^2\frac{\theta}{2} - \frac{3}{2}k_2 \sin\theta\right] \tag{3}$$

$$\tau_{r\theta} = \frac{1}{2\sqrt{2r}} \cos\frac{\theta}{2}\left[k_1 \sin\theta + k_2(3\cos\theta - 1)\right]$$

where for a constant uniaxial tensile loading the stress intensity factors for extension are $k_1 = \sigma_0\sqrt{a}$ and $k_2 = 0$.

Superimposing the results of equations (1) and (3) gives the resultant stresses near the crack due to the combined loading:

$$\sigma_r = \frac{1}{\sqrt{2r}}\cos\frac{\theta}{2}\,k_1(1+\sin^2\frac{\theta}{2}) + \frac{3\delta K_2}{h\sqrt{2r}}\sin\theta\,\cos\frac{\theta}{2} + \frac{2\delta}{h\sqrt{2r}}\cos\frac{\theta}{2}\,K_1(1+\sin\frac{\theta}{2})$$

$$\sigma_\theta = \frac{1}{\sqrt{2r}}\cos\frac{\theta}{2}(k_1\cos^2\frac{\theta}{2}) - \frac{3\delta K_2}{h\sqrt{2r}}\sin\theta\,\cos\frac{\theta}{2} + \frac{2\delta}{h\sqrt{2r}}\cos^3\frac{\theta}{2}\,K_1$$

$$\tau_{r\theta} = \frac{1}{2\sqrt{2r}}\cos\frac{\theta}{2}(k_1\sin\theta) + \frac{2\delta K_2}{h\sqrt{2r}}\cos\frac{\theta}{2}(3\cos\theta - 1) + \frac{2\delta}{h\sqrt{2r}}K_1\cos\frac{\theta}{2}\sin\theta \qquad (4)$$

There are two problems that immediately arise. First, the physical limitations of experimentation may make it impossible to follow the assumption of an infinite plate. Thus, the value of K_1 cannot be assumed to be zero. The second problem is that each of the stress equations is seen to be composed of three components: the static component due to k_1, and the dynamic components due to K_1 and K_2. While it is known that the crack cannot grow under the static tensile loading, it would be unreasonable to neglect its effect in this combined loading situation.

In an effort to overcome the second problem, the mechanism proposed by Schijve [7] may be profitably utilized. Schijve has explained that crack extension may be thought of as a geometric consequence of dislocation movements. He recognizes two separate mechanisms of dislocation movements. The first of these is believed to be the controlling factor for slow growth rates and even for

crack nucleation. In this dislocation-absorption mechanism the dislocations move towards the crack and travel into the tip region. The second mechanism, the dislocation-generation mechanism, is present when high growth rates occur. Here the dislocations are believed to form at the crack tip region due to the presence of large shear stresses. One or both of these mechanisms may occur at any time. These dislocations may then be used to formulate a crack propagation law of the form [7]

$$\frac{da}{dN} = \phi m b \tag{5}$$

where m is the total number of dislocations, b the magnitude of Burgers vector and ϕ the number of active dislocations.

Since it is assumed that the dislocation movements will all be within the plastic zone, m can be thought of as a function of the plastic zone size p:

$$m = f_1(p) \tag{6}$$

It has been further hypothesized that ϕ also may be expressed as a function of p: [3]

$$\phi = f_2(p) \tag{7}$$

These functions are generally monotonic increasing functions which vanish at p = 0. Therefore, if the range of p is kept sufficiently small, f_1 and f_2 may be approximated by power series. [2] Thus, the rate of crack growth can be expressed in the form:

$$\frac{da}{dN} = A_1 p^{\alpha_1} A_2 p^{\alpha_2} \tag{8}$$

It is important that the function be expressed in this manner since it may allow the consideration of the effects of both the static load and the dynamic loads simultaneously. This is because m, the total number of dislocations, should be based on the maximum plastic zone size, which might be assumed to be the sum of the plastic zones due to tension and bending. The fraction of dislocations involved in the crack extension may depend only on the active section of the total plastic zone caused by the fluctuating bending loads. Thus, the rate of crack extension might be expressed as

$$\frac{da}{dN} = A(p_e + p_b)^{\alpha_1} (p_b)^{\alpha_2} \tag{9}$$

The value of p_e, the plastic zone size for plane extension, has been realistically estimated by Dugdale [8] to be

$$p_e = \left[\sec \frac{\pi \sigma_o}{2 \sigma_y} - 1\right] a \tag{10}$$

which may be simplified by the first term approximation for small values of $\frac{\sigma_o}{\sigma_y}$ to

$$p = \frac{1}{2} \left(\frac{\pi \sigma_o}{2 \sigma_y}\right)^2 a = \frac{1}{2} \left(\frac{\pi}{2 \sigma_y}\right)^2 k_1^2 \tag{11}$$

The case of cylindrical bending has been estimated by Erdogan and Roberts [2] using reasoning similar to that of Dugdale. They found that by assuming the plate to be elastic except for a rigid plastic zone near the crack tip and calculating the stresses and moment

distributions at the crack tip, the plastic zone size can be expressed as

$$p_{bs} = a\left(\sec\left(\frac{\pi \sigma_b^o}{4\sigma_y}\right) - 1\right) \quad (12)$$

This equation can be simplified for small values of $\frac{\sigma_b^o}{\sigma_y}$ by the first term approximation

$$p_{bs} = \frac{1}{2}\left(\frac{\pi \sigma_b^o}{4\sigma_y}\right)^2 a = \frac{1}{2}\left(\frac{\pi}{4\sigma_y}\right)^2 K_1^2 \quad (13)$$

where K_1 is the stress intensity factor for symmetric bending.

Since equation (11) has been shown to be valid for both the symmetric and skew-symmetric stress intensity factors for extension, it would be expected that equation (13) would be true for both the symmetric and skew-symmetric stress intensity factors for bending. Proceeding under the above assumption it is possible to formulate a power law of the form of equation (9). By continued use of the assumption that the plastic zone sizes from different effects may be additive, the expression for the plastic zone p_b can be written as

$$p_b = \frac{1}{2}\left(\frac{\pi}{4\sigma_y}\right)^2 (K_1^2 + K_2^2) \quad . \quad (14)$$

Substitution of equations (11) and (14) into equation (8) yields the result

$$\frac{dA}{dN} = A\,\frac{1}{2}\left(\frac{\pi}{4\sigma_y}\right)^{2\alpha_1+\alpha_2} (K_1^2 + K_2^2 + 4k_1^2)^{\alpha_1} (K_1^2 + K_2^2)^{\alpha_2} \quad , \quad (15)$$

which may be simplified for small ranges of p to

$$\frac{dA}{dN} = B(K_1^2 + K_2^2 + k_1^2)^{\alpha_1} (K_1^2 + K_2^2)^{\alpha_2} \quad (16)$$

Equation (16), which expresses the rate of crack extension as a function of the stress intensity factors involved, is in the general form often used in the literature.

As a point of interest, the stress at the crack tip may be determined from equation (4) and used in a Mohr circle analysis. For the special case of a surface element located at the coordinate $(a + \frac{1}{2}, 0)$, the stresses at the time of zero shear load are

$$\sigma_r = k_1 , \qquad \sigma_\theta = k_1 , \qquad \tau_{r\theta} = 0 .$$

When the shear load Q is at its maximum value the stresses are

$$\sigma_r = k_1 + K_1 , \qquad \sigma_\theta = k_1 + K_1 , \qquad \tau_{r\theta} = K_2 .$$

From this it may be seen that the mohr circle would start as a point when Q = 0 and expand to some maximum diameter when Q reaches its maximum. It also may be observed that the center of the circle is translated through the distance k_1, (see Figure 6).

The principal stresses in this case are always located at $\pm 45^\circ$ from the horizontal, and they are equal in magnitude to $k_1 + K_1 \pm K_2$.

III. Design of the Machine

The machine, as it was originally conceived, was to supply a constant displacement to the edge of the initiating crack near its center. A number of mechanical systems to provide the constant displacement were considered, but these were all disregarded when it was decided to choose a sinusoidal loading of constant amplitude in order to substantiate the existing theory. A number of ways to achieve this type of loading were considered. They ranged from pneumatic cylinders and spring systems to eccentric discs of the type that were finally adopted.

The loading device about which the entire machine is designed is quite simple, (see Figure 7a). It consists of a simple vertical lever pivoted in the middle. The top of the lever is connected to the plate through a slender member so that the crack could be easily observed. An eccentric which is located at the bottom of the pivot, spins in the plane perpendicular to the plate. As the eccentric is turned at a constant speed, there is a rotating force of constant magnitude. The horizontal component of this force is transmitted to the plate, while the vertical component is carried by the frame, (Figure 7b). It is obvious that the desired sinusoidal loading would be supplied to the plate, if the plate deflection at the point of load application were small. Under this restriction, the load would be proportional to the square of the speed of rotation[1]. The magnitude of the loading in

(1) Actual speed vs. load characteristics can be found in Appendix B.

such a system can be varied in two ways; by increasing the number or size of the eccentric weights, and by varying the speed. Since the deflections of the plate in the region of the shear load application were expected to be quite large, some nonlinearities in the loading system due to the large inertia of the pivot arm and eccentric were anticipated. It was felt, however, that these would have a small effect. The deflection of the plate would, of course, vary with crack length so these nonlinearities could cause a change in the maximum force attained at a given speed, but the force could be easily held constant by varying the operating frequency. This change in frequency, especially such a small one, has been found to have no effect on the rate of crack extension,[1] and, therefore, there can be no objection to changing the frequency as an excellent method of maintaining the constant maximum load desired. In the interest of limiting the previously mentioned nonlinearities, the moment of inertia of the linkages constituting the loading system is kept as small as possible. This was accomplished by machining as much excess material as possible from the solid steel bar which had to be used to eliminate the stress concentrations inherent in a member fabricated by welding.[2] Unfortunately, large secondary dynamic forces resulted in the load curve shown in Figure 8 when light Torrington Needle Bearings were used at all the pin connections shown in Figure 7. A subsequent design with heavy bronze bushings eliminated this problem and gave the more desireable

(2) The determination of the dimensions is presented in Appendix A.

load curve shown in Figure 9. The moment of inertia of the loading device is made considerably greater by the rather large eccentrics, and by the 1/4" thick aluminum discs to which the eccentrics are attached. The discs, however, are necessary since they play a dual role of providing safety for the operator and of assuring alignment of the two eccentrics, which are located symmetrically about the pivot arm for balance, (Figure 10). The drive linkage from the stationary motor to the moving loading mechanism is made by means of flex-shaft.

The member that transmits the loading from the pivot arm to the plate as originally conceived was one piece of 3/8" drill rod. It was to be connected to the plate through both tensile and compressive phases of the loading by a 4-40 socket head cap screw. Ball bearings drilled to fit on the cap screw on either side of the plate were used to reduce the bending moment transmitted to the plate, (Figure 11).

During subsequent use of the machine it became obvious that there was still a large bending moment present, since the cap screws were exhibiting bending fatigue failure. The design adopted to circumvent this problem is simply a short clevis placed at the plate end of the member, (Figure 12a). With this clevis in place the bending moment at the plate is very small since the distance of misalignment "d" will be small, (Figure 12b). The inaccuracy of the previous assumption of a pin connection is further emphasized by the fact that the same ball bearing pivot used in the first design is now used as an approximation of a solid connection.

The machine used in the testing presented in this report only has one such eccentric drive. The second "Q" force is supplied by a fixed arm. Since the boundaries of the plate are not infinite, this situation

does not provide the symmetric loading that was discussed theoretically. Therefore, the author has designed a system of timing belts that will allow a second eccentric to be driven in phase with the first, (Figure 13). This will provide the symmetric transverse shear loading. The eccentric system as shown, with both shafts rotating in the same direction, will create a large rocking unbalance, so the frame must be massive and firmly mounted to the floor.

As was mentioned before in order to force the crack to grow in a straight horizontal path that could be easily measured, a tensile load perpendicular to the initiating crack is employed. This load is of the magnitude of 10,000 pounds. The possibility of cycling the tensile load was also considered in the design of the machine.

The design of the frame is very straight forward. It is such that the large forces due to the tensile load are contained in as few of the members of the frame as possible, thus keeping the size of the frame small. A yoke of 4" steel channel placed back to back to form "I beams" supports the 10,000 pound maximum loading, and provides pivot points for the lever system employed to transmit the force to the plate, (Figure 14).

The jaws that support the plate are massive to provide a fairly even distribution of the tension loading across the plate[3], (see Figure 15). The bottom jaw is constrained from motion in the transverse

(3) The actual strain distributions are shown in Appendix C.

direction by retractable cam rollers, which allow strain of the plate during a cyclic tensile loading. The jaws, therefore, provide fixed boundary conditions for the two edges of the plate parallel to the initiating crack. If simply supported edges are desired on all edges of the plate this may be achieved by the simple modifications of retracting the cam rollers, and placing spherical bearings at the pin connections in the jaws. It is noteworthy that the tensile force is transmitted from the jaws to the plate by friction since the jaws have been roughened. The normal force is supplied by tightening the seven 3/8" bolts on each jaw.

The rest of the framework merely supports the yoke and provides a base for the loading eccentrics and their driving equipment. The frame support is symmetric to allow the later addition of the second eccentric and the timing belts, and is bolted to the floor so that the frame cannot vibrate due to the large unbalance created by the spinning eccentrics. Figure 16 shows various photographs of the completed machine.

Some of the features of the design may be of interest. The transverse loading eccentric uses bronze bushings throughout. The tensile loading levers have Torrington Needle Bearings (numbers: HJ42212 and HJ-101812) at the pivot points and Heim Uniball Spherical Bearings at all lever pins. The lower jaws are constrained by Torrington No. CR12 cam rollers. The motor is of the 1/2 horsepower variable speed, direct current type.

IV. Details of Operation

The plate should first be prepared for testing. A plate of any thickness up to and including 0.1" may be successfully tested on the machine. The specimen should be cut and drilled according to Figure 17. The initiating crack is cut in the plate with a jewelers saw. Since the initiating cracks are sometimes quite long, it becomes necessary to clamp old parallels a sawblade width apart to guide the blade in a straight path. The actual crack tip is made by placing a single edge razor blade in the saw cut and striking it with a sharp hammer blow.

Preparation of the plate surface for easy observation of the crack is essential. The guiding rule for any type of polishing is to buff the plate in the direction perpendicular to that of the expected crack growth. If this procedure is not followed extremely inaccurate crack length readings will result. Polishing the specimen on a buffing wheel gave the best results in the tests conducted. When this method is employed even the very fine tip of a long crack could be instantly identified. DuPont "7" rubbing compound normally used in testing of this type, resulted in less distinct crack tips and large experimental error.

The plate may be conveniently placed on the machine if the following procedure is used. The top front jaw should be completely removed from the machine, and the bottom jaws should be held in a horizontal position with pieces of angle iron wedged between the ends of the jaws and the frame. These wedges are used to keep the jaws from rotating out of position. The plate is then placed in between the bottom jaws and bolted in place loosely by the two end 3/8" socket

head cap screws. The front top jaw may then be put in place, and holes in the jaws aligned with those in the plate by manipulation of the tensile loading lever. Again this is most easily accomplished by use of the two end bolts. After the other bolts are in place the load lever should be fully raised so that the plate is placed in a slight compressive load. This is done to assure that when the bolts are tightened none of them will be in contact with the plate. The whole tensile load then will have to be carried by friction rather than by bearing on the plate. All the bolts should be tightened with the same torque so that the tensile stress field in the plate will be uniform and symmetrical. At this point the cam rollers would be brought into contact with the jaws, if the fixed boundary condition were desired.

The loading device is next connected to the plate with the 4-40 cap screws as previously described. They should be tightened just enough to eliminate any play which would make the loading erratic, but not so tight as to crush the plate (Figure 18), since the crushing of the plate around the cap screws contributes to the problem of short fatigue life of the screws.

The tensile load at the present time is a constant load and is applied by a dead weight. The loading is measured by a type A-5 SR4 strain gage (gage factor 2.03, gage resistance 120 Ω). This gage is placed on the lower tension member between the jaws and the first lever. (See Figure 14) This position was chosen for the gage to eliminate the effect of friction in the lever bearings as much as possible. This strain is measured by static strain equipment like the Baldwin Lima

Hamilton Model K. The dynamic loading is measured by two type C-11 strain gages (gage factor 3.2, gage resistance 300 Ω) placed on opposite sides of the 3/8" diameter loading rod to eliminate any possible false readings due to bending. Two more gages of this type are used as dummy gages to complete the four arm bridge. The bridge is connected to a type Q plug in unit in a type 535 Tektronix Oscilloscope.

The microscope, which is a 50 power Gartner Traveling Microscope, is most easily mounted on a stand as shown in Figure 16. This author found it best to light the specimen with a 40 watt-fluorescent lamp located below the microscope so the light would reflect from the plate into the microscope. This arrangement had the advantages of having no glare and allowing, at least on a polished plate, an accurate determination of the crack length with a minimum motion of the lamp to eliminate the shadows.

Operation of the machine is accomplished by adjustment of the motor speed potentiometer until the required deflection appears on the oscilloscope. The number of cycles can be read on the electric counter, which may be reset to zero at any time.

The most satisfactory data seems to be gathered if the tip-to-tip crack length readings are taken at about .05" crack growth intervals. This interval gives a sufficient number of points to plot a smooth curve and also allows the number of cycles between readings to be large enough so that the percentage of error in the number of cycles is low. The percent of error is quite large for runs of a few cycles since the loading device is slow in starting and stopping.

V. Experimental Results

Preliminary tests have been performed on three plates. In all cases the horizontal plate edges were fixed, and the fluctuating load Q was supplied to only the top crack edge. The bottom crack edge was held fixed by an arm mounted on the frame of the machine. All of the tests were performed with a fluctuating transverse shear load with a maximum amplitude of $157^{\#}$ and a static tensile load of $10{,}000^{\#}$. Three different initial crack lengths have been used. Those, and the results of the testing, may be found in Figures 19, 20, and 21.

A review of the three growth curves indicates that each crack exhibits a short period of increasing crack growth rate followed by a long period of decreasing crack growth rate. It may be noted that the length of the crack at the start of the test had no observable effect on the size of the zone of accelerating crack growth, and it should be stated that under the test conditions described above crack extension virtually stops as the crack length approaches $3\frac{1}{2}"$.

It was hoped that there would be no interference of the crack edge on itself, but the three test plates have shown this assumption to be incorrect. Evidence of the interference of the crack edge on itself is found in the appearance of the crack surface that has been cut apart after testing. Each side of the crack appears to have grown inward from the plate surface to the plate center independent of the other side in such a manner that the two "crack halves" do not meet. This results in a small step in the crack surface which would make interference unavoidable in any reversed shear loading situation.

The direction of crack growth is noted to be the same in all three tests. The crack starts to grow in line with the initiating crack, but it gradually curves away from the fixed side as is shown in Figure 22.

The second and third plates tested exhibit smooth growth curves. These plates both have highly polished surfaces which allows accurate crack length data to be obtained on an unloaded plate.

The appearance of the crack varies during the course of the test. Near the initiating crack the plate appears to undergo cold work, and the crack has many visible branches. As the crack gets longer, however, the change in the plate surface appearance caused by the cold work disappears, and there is less branching present.

In an effort to determine the symmetric bending moment on the plate two strain gages were placed in the center of the plate near the top fixed edge. The surface stress on a plate during a fatigue test with the load conditions previously described is observed to have a peak to peak variation of 2,100 PSI, when the crack is 1" long.

A final test was performed on a plate in which neither the fixed support not the cam roller constraints were employed. Application of a transverse shear force of 157# and a tensile force of 10,000# to an initiating crack resulted in a very small growth rate. This crack grew immediately in a direction about 30° from the initiating crack (see Figure 23).

VI. Discussion and Conclusions

The discussion in section II indicates that the rate of crack extension should be a function of the stress intensity factor raised to some positive power. The results of this investigation indicate a decreasing growth rate, except in the close proximity of the initiating crack. Unfortunately the region with accelerating crack growth is too short to yield any useful results.

This deviation from the expected result may be explained by a careful consideration of the differences in the actual test situation and the theoretical model.

The first important difference is the lack of the symmetric transverse shear loading that was used in the derivation of equation (2). While this in itself should not cause a decreasing crack growth rate, it is still desirable to have the symmetric loading system for two reasons. First, the symmetric case is of greater theoretical significance; and second, the lack of symmetry may be the reason that the crack does not grow in a straight line. This situation is being rectified by the construction of the second loading eccentric as previously discussed.

The theory discussed assumes an infinite plate. The tests described in this report utilized a small plate with two edges fixed. The fixed supports could possibly reduce the rate of crack growth by carrying progressively more of the transverse shear force load in bending as the crack gets longer. This also complicates the theoretical solution by introducing symmetric bending into the problem. This effect is small, however, since experimentation has demonstrated that for a 1" crack the stress intensity factor is only 1.05×10^3 lb/in $^{\frac{3}{2}}$. For For the same test conditions $K_2 = 30.0 \times 10^3$ lb/in $^{\frac{3}{2}}$ and $k_1 = 5.90 \times 10^3$ lb/in $^{\frac{3}{2}}$.

The problems posed by the fixed jaws will be reduced to some extent when the jaws are pivoted on spherical bearings.

The interference of the crack on itself is probably the major factor in the decelerating rate of crack extension. As the crack gets longer the area of the crack surface that is rubbing on itself gets larger, and more of the force is transmitted to the opposite crack surface along the length of the crack instead of in the area of the crack tip. It is possible that if the crack were cycled long enough, the crack would stop all growth. This would seem to indicate that cracks of this type should not be very troublesome, since they are self-arresting. While crack growth with interference is certainly an important problem that might be handled theoretically by an assumption of the friction force as a function of crack length, it is still important to be able to eliminate the interference as much as possible in order to determine the validity of the present theory. While the interference may not be eliminated, it may be reduced to a minimum by removal of the plate material with a jeweler's saw up to within 1/4" of the crack tip. If this procedure is followed there will never be much more than 1/2" of crack interference.

The sinusoidal form of the transverse shear load that has been achieved demonstrates that the eccentric type loading mechanism can provide the loading that is required for many different types of experimentation. Because of the success of this loading system, the additional investment is being made in the second loading arm which will make it possible to provide a symmetric loading capability of the type discussed in the section on Theoretical Considerations.

The testing performed is entirely of a preliminary nature. Even though all the useful data indicated a decreasing rate of crack growth, it must be remembered that this was probably caused by the unsymmetric loading, the fixed end conditions of the plate, and the interference of the crack edge on itself. As was explained, all of these problems can be reduced by the addition of the second load lever, changing the jaw pin connections to spherical bearings, and cutting away the material at the crack edge which was causing the interference. When these changes are completed experiments will probably show the increasing rate of crack growth anticipated.

When the final addition to the machine, a device to vary the tensile force with time, is complete, the machine will be extremely versatile, as there will be the added ability to cycle the tensile load in phase with the transverse shear load.

It is obvious that a great deal of both experimental and theoretical work will be required before any truly satisfactory answers to the problem are found.

APPENDIX A

Determination of the More Important Dimensions of the Machine

The entire design is based on the knowledge that the eccentric type loading system previously described would be used for testing plates of the size 18" by 12".

The first step was the determination of the forces required to crack the plate. For plates of less than 0.10" thickness the maximum loading required for crack growth can be found from Equation 2 and

$$K_2 = \frac{6Q\sqrt{a}}{h^2} \qquad (2)$$

the fact that crack extension occurs at values of K_2 greater than $K_{cr} = 30{,}000$. Rearranging equation 2 and making the appropriate substitutions yields a value of $Q = 157^{\#}$. Since it is felt a slight factor of safety should be used, a loading of $200^{\#}$ is used as the design load. The tensile loading of $10{,}000^{\#}$ is felt to be of sufficient magnitude to control the direction of the crack growth.

The loading pivot arm (Figure 24) is symmetric about its center and 18" long since this size fits the requirement of allowing two eccentrics to be placed below table level conveniently and safely.

The original arm that was used proved to be unsatisfactory because it was not rigid enough, even though it satisfied all bending stress requirements. Consequently there is no use considering the stresses present in the new heavier pivot arm.

The eccentrics are made in the odd shape shown in Figure 25 so that they could be kept as small as possible, and still provide the required load. Once the shape is determined and the center of gravity

$\bar{r}$ is found experimentally it is a simple matter to determine the thickness of eccentric required. For steel having a specific weight of .283 lb/in^3 and $\bar{r} = 3.55"$ at a maximum speed n = 900 RPM or 94.2 Rad/sec

$$Q = mn^2\bar{r} = \frac{(14)(3.55)(94.2)^2(.283)}{386} = 320^{\#}$$

for each inch thickness of steel eccentric. Thus for any load and speed combination the proper thickness of the eccentric weights can be determined.

Since, even a 1/4" diameter rod would be satisfactory from the buckling standpoint, the 3/8" diameter drill rod finally chosen for the member connecting the plate to the loading pivot is more than adequate. The small clevis at the end near the plate, however, bears some discussion (Figure 26). Even though the stress levels in bearing on the 3/16" pin are extremely low, the two legs must be quite sturdy as shown or the clevis will "spring" and the pin will soon wear the holes in the clevis to the extent that the entire sinusoidal load pattern will be lost.

The entire frame structure is designed around the 10,000 lb. load. This is the only loading that caused any serious stress problems. As is previously mentioned a yoke is employed to keep the large forces in as small a portion of the total frame as possible. The 4" channels are used for the yoke as they satisfy the dual requirement of carrying the load and allowing the use of the 2 x 3/4" steel tension members to the jaws. The highest stress in the horizontal channel sections is

$$\sigma_b = \frac{M_c}{I} = \frac{65{,}000(2)}{2(3.8)} = 17{,}100 \text{ PSI}$$

which is quite low, and the critical load for buckling is

$$P_{cr} = \frac{\pi^2 EI}{2} = \frac{(3.14)^2(3 \times 10^7)(.64)}{(3.8)^2 10^2} = 1.31 \times 10^5 \text{ lbs.}$$

so there should be no buckling problem.

The 10,000 lb. loading is supplied by 100# transmitted by two levers in series. Each has a length ratio of ten to one, and is made in essentially the same manner. The heavy set of levers is composed of two 2 x 3/4" cold rolled steel bars side by side with a 3/4" gap between them for the tension members and the pivot. Pins of 1/2" diameter are used in the short end of the lever and these must each withstand a shear stress of 26,600 PSI, while the lever withstands a maximum bending stress of less than 20,000 PSI even when a stress concentration factor of three is used. In order to maintain the small overall size of the frame it is necessary to use levers only 22" long. Thus the pin distance at the short end of the lever is only 2". This is the only cause of stress carrying difficulties in the design. The small distance between the two pins makes it impossible to use a tension member from the lever to the lower jaw any larger than two inches wide. The thickness of this member is controlled by the gap in the yoke and cannot be any thicker than 3/4". Under the original design this presented no difficulty, but under the present modifications where a bulky spherical bearing is included to eliminate any problems of misalignment, the stress level is 29,400 PSI where a stress concentration factor of 2.2 is used and there is no consideration of

any factor of safety. For this reason cold rolled 1015 steel with a yield stress of 55,000 PSI is used. This steel, however, will not be adequate for the possible future varying tensile load since fatigue will have to be taken into consideration. For this application the endurance limit of the material should be of the magnitude of 40,000 PSI so the ultimate strength must be above 80,000 PSI. The author obtained such a piece of stock but has been unable to get it machined. The other tension members and lever set are under such low stress levels that they are not worth considering at this time.

The rest of the machine posed no difficulties at all. The entire frame and its table are of welded construction. and all the components are picked and located for convenience of construction or operation.

APPENDIX B

Calibration Curve for the Transverse Shear Load Q

The load speed curve presented in Figure 27 was determined using a 0.10" 2024-T3 bare aluminum plate with no crack. The speed required to obtain certain loads is presented below and an attempt to formulate an equation for the curve is shown.

Table I

Load (lbs)	Speed (RPM)	Load (lbs)	Speed (RPM)
33	200	233	525
66	272	266	560
100	345	300	585
133	387	333	625
166	440	366	650
200	475	400	675

From dynamics, the load will be proportional to the square of the speed,

$$Q = Kn^2$$

The correct value for K may be found by use of the method of least squares in conjunction with the information in Table I.

Set

$$A = \sum_{1}^{N} (Q_i - Kn_i^2)^2 = \text{minimum}$$

To find the minimum above let,

$$\frac{A}{K} = 0$$

or

$$-\sum_{1}^{N} 2(Q_i - Kn_i^2)\,2n_i = 0$$

which is the same as

$$\sum_{1}^{N}(Q_i - K_i n_i^2)\,n_i = 0$$

so

$$\sum_{1}^{N}(Q_i n_i) = \sum_{1}^{N} Kn_i^3$$

and finally,

$$K = \frac{\sum_{1}^{N} Q_i n_i}{\sum_{1}^{N} n_i^3}$$

The value for K can be calculated to be .785 from the above data. So,

$$Q = .785\ n^2$$

A curve of actual eccentric speed vs. crack length which was made during the test of plate II is shown as Figure 28 . This curve is of special interest since it reflects the importance of the previously mentioned non-linearities that occur with plate deflection.

APPENDIX C
Strain Distribution on a Plate Under Test

A plate of 2024-T3 bare aluminum .1" thick, was subjected to a fatigue test. It was placed under a 10,000 lb. tensile load, and subjected to a Q force of 157#. Type A-5 SR-4 strain gages were located as shown in Figure 28. The following strains were found at various crack lengths.

Table II

2a in	in/in	in/in	in/in	in/in	in/in	
1.55565	360	510	445	295	345	
1.71245	350	520	450	360	340	
1.73290	340	520	450	365	330	
1.75440	330	520	445	360	310	
1.81565	330	525	450	360	310	
1.83910	310	570	495	360	310	
1.86505	350	560	445	350	335	Reading done on different day
1.96410	350	540	470	365	345	
2.07170	345	550	470	378	350	
2.20040	330	550	470	370	338	
2.30735	335	565	485	385	345	
2.42315	330	575	490	390	335	
2.48835	330	580	495	400	320	
2.54950	325	583	500	400	320	
2.60120	310	580	490	380	340	
2.68675	310	590	500	390	340	
2.74180	305	570	480	380	330	

cont.

Table II (cont.)

2.79155	300	578	487	380	330
2.87335	290	575	485	380	330
2.95895	295	570	485	380	330
3.01830	300	570	490	390	335
3.19360	275	570	480	370	320
3.29720	230	570	485	380	315

The above strains indicate that the desired uniform stress field is not present, since the strain near the edge of the plate is smaller than would be expected even considering the Poisson effect. It is difficult to believe that the large jaws previously discussed could be responsible for this. The low strain at the edge of the plate could be due to insufficient roughness of the jaw faces which resulted in the plate slipping slightly under loading.

APPENDIX D

Crack Growth Data

The data that follows is the result of three tests that were all performed on 0.10" 2024T3 bare aluminum plates with a Q load of 157# and of a tensile load of 10,000#.

Plate I

No. of Cycles (N)	Crack Length 2a	Comments
0	1.55565	
1,000	same	
2,000	1.59680	
2,250	1.71245	
2,450	1.73290	
2,750	1.75440	
3,050	1.81565	
3,350	1.83910	
3,660	1.86505	
3,960	1.88580	
4,260	1.91395	
4,560	1.94445	
5,160	1.96410	Note scope turned right side up.
5,460	2.00790	
5,760	2.03867	
6,100	2.07170	
6,400	2.09890	
6,700	2.11920	
7,000	2.15690	

(cont.)

Plate I (cont.)

No. of Cycles (N)	Crack Length 2a	Comments
7,300	2.20040	
7,600	2.23890	
7,900	2.25180	
8,200	2.28960	Tip unconnected from main crack
8,500	2.30735	
8,800	2.34100	
9,100	2.37635	
9,400	2.40150	
9,700	2.42315	
10,000	2.45355	
10,300	2.46650	
10,600	2.47170	
10,900	2.48435	
11,200	2.50345	
11,700	2.52680	
12,400	2.54950	
13,400	2.60120	
14,400	2.64355	
15,400	2.68675	
16,400	2.74180	
17,400	2.74870	
18,410	2.77500	
19,410	2.79155	
20,410	2.80285	

(cont.)

Plate I (cont.)

No. of Cycles (N)	Crack Length 2a	Comments
22,410	2.82211	
24,410	2.87335	
26,410	2.91100	
28,410	2.94610	Left hand side growing slowly, crack interfering with itself.
30,910	2.95895	
33,910	2.96570	
38,910	3.01830	
43,910	3.03470	
48,910	3.05865	
58,910	3.09765	
68,910	3.19360	Loose capscrew due to plate cracking at mount. Load distribution not sinusoidal
73,910	3.20020	
78,910	3.21445	
88,910	3.26785	
98,910	3.27355	
108,910	3.28435	
118,910	3.29720	

Plate II

No. of Cycles (N)	Crack Length 2a	Comments
0	1.30990	
300	1.33280	Left end of crack can not be located due to scratch in plate.
600	1.35430	
900	1.37480	
1,200	1.40445	High load, much branching.
1,500	1.44990	Cold work around the crack.
1,800	1.50435	
2,100	1.56330	
2,400	1.61660	
2,700	1.68220	
3,000	1.72980	
3,300	1.79900	
3,600	1.84925	
3,900	1.89290	
4,200	1.94240	
4,500	2.00320	
4,800	2.04965	
5,100	2.09095	
5,400	2.12595	
5,700	2.16570	
6,030	2.19960	
6,330	2.22240	
6,630	2.24300	

(cont.)

Plate II (cont.)

No. of Cycles (N)	Crack Length 2a	Comments
7,130	2.28370	
7,630	2.33065	
8,130	2.36485	
8,700	2.41160	
9,300	2.44870	
9,900	2.48730	
10,500	2.52200	
11,100	2.55260	
12,000	2.58860	
13,000	2.62345	Loading difficulties (Change) (Loading)
14,000	2.64800	
15,000	1.20950	
16,000	1.19570	
17,000	1.18590	
18,500	.58570	
20,000	.56950	
21,510	.55295	
24,000	.54190	
27,000	.52520	
31,000	.50490	
36,000	.53715	
44,000	.51740	
54,000	.49300	
69,000	.47915	
84,000	.46140	

(cont.)

Plate II (cont.)

No. of Cycles (N)	Crack Length 2a	Comments
99,000	.48340	
114,000	.47175	
129,000	.45190	Roughness in operation noted.

Plate III

No. of Cycles (N)	Crack Length	Comments
0	1.01105	
300	1.01280	
600	.98445	
900	1.01500	
1,200	1.00360	
1,500	.98200	
1,800	.96290	
2,100	.94410	
2,400	.92310	
2,700	.89970	
3,000	.88865	
3,300	.87880	
3,600	.86400	
4,100	.83735	
4,610	.81055	
5,110	.79325	
5,700	.77310	
6,200	.75350	
6,700	.73510	
7,200	.72000	
7,900	.64265	
8,600	.62860	
9,300	.61525	
10,000	.59670	

(cont.)

Plate III (cont.)

No. of Cycles (N)	Crack Length	Comments
11,000	.95350	
12,500	.93470	
14,000	.92785	
16,000	.90260	
18,000	.89180	
20,000	.88220	
24,000	.86895	
28,000	.84820	
32,000	.83430	
36,000	.81985	
44,000	.79270	Right tip of crack growing vertically downward.
59,000	.76010	
81,000	.73480	Still vertical

Test ended because right crack tip has almost stopped growth.

APPENDIX E

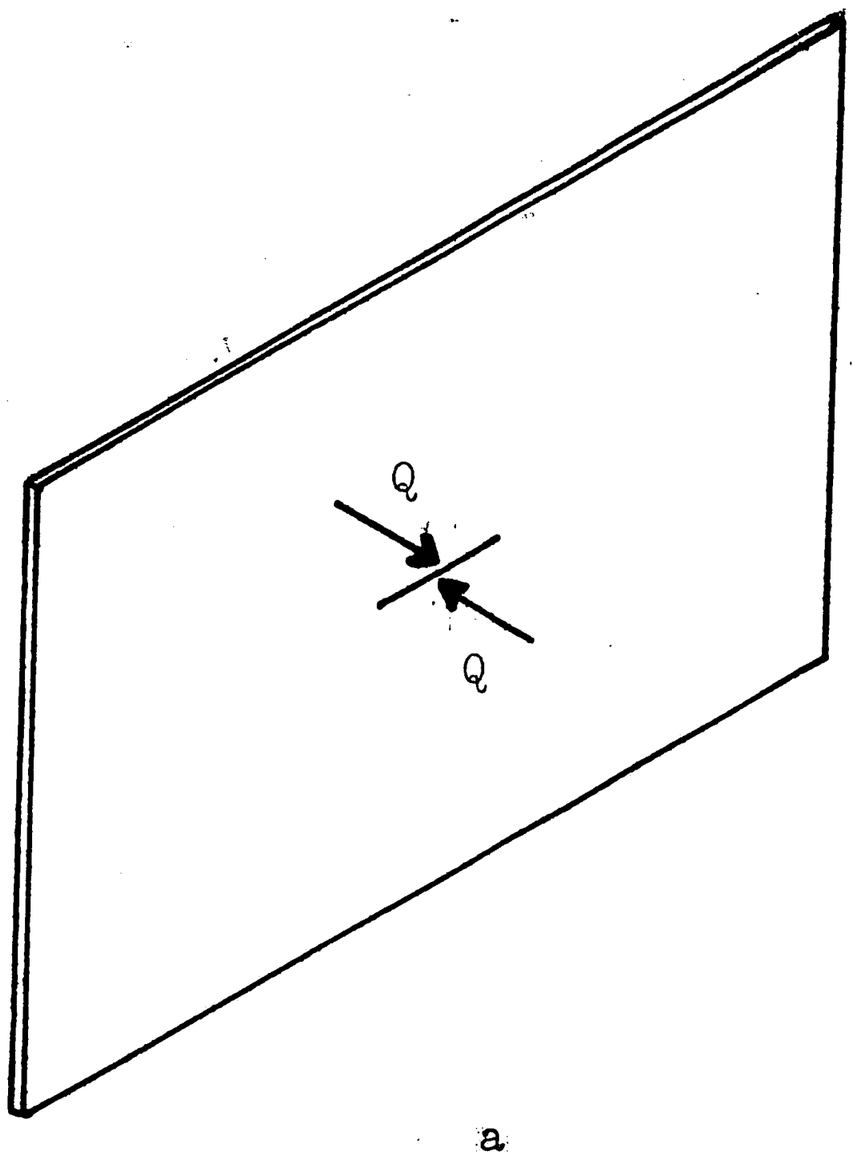

a

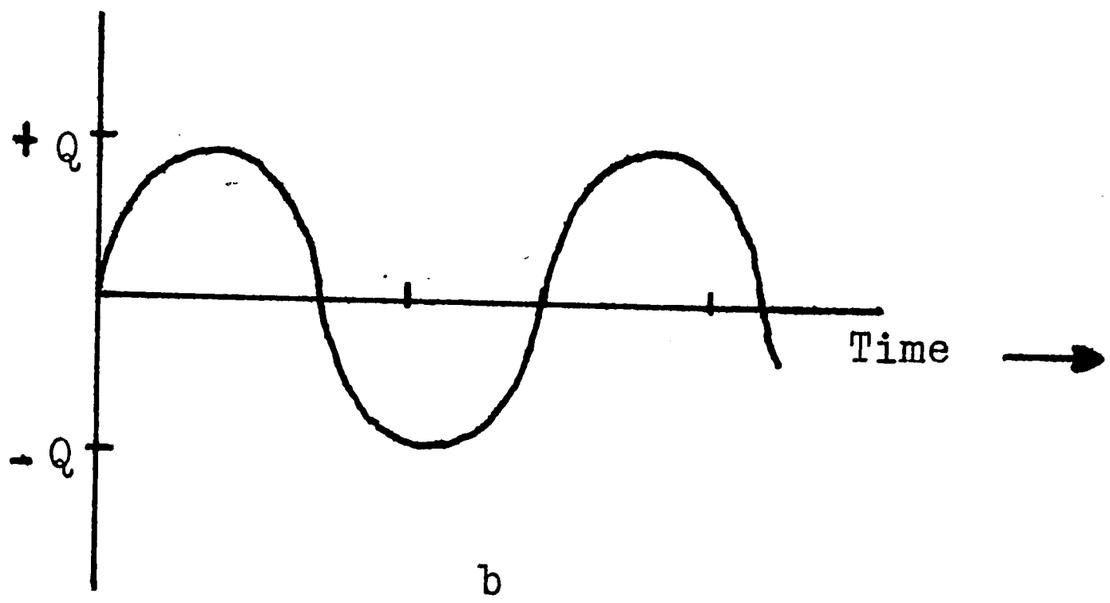

b

Figure 1

Transverse Shear Loading Applied Near the Initiating Crack and the Load Variation With Time

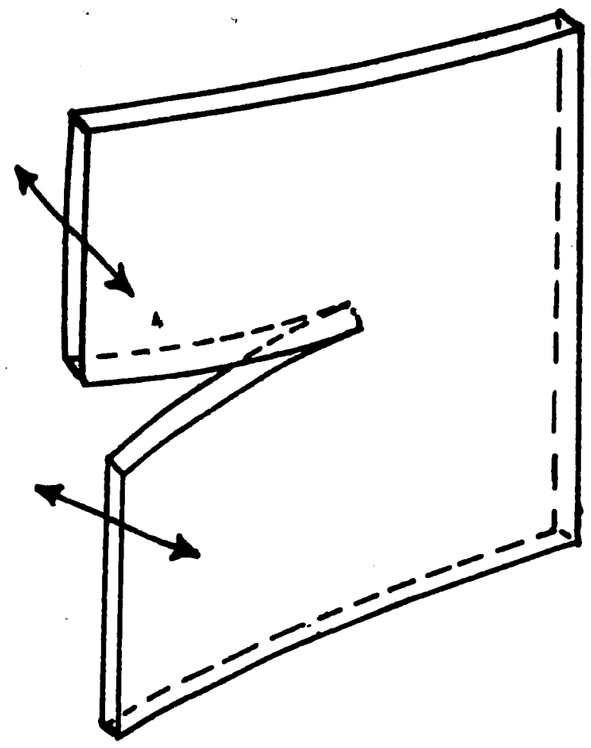

Figure 2

A Crack Tip Undergoing Bending Fatigue

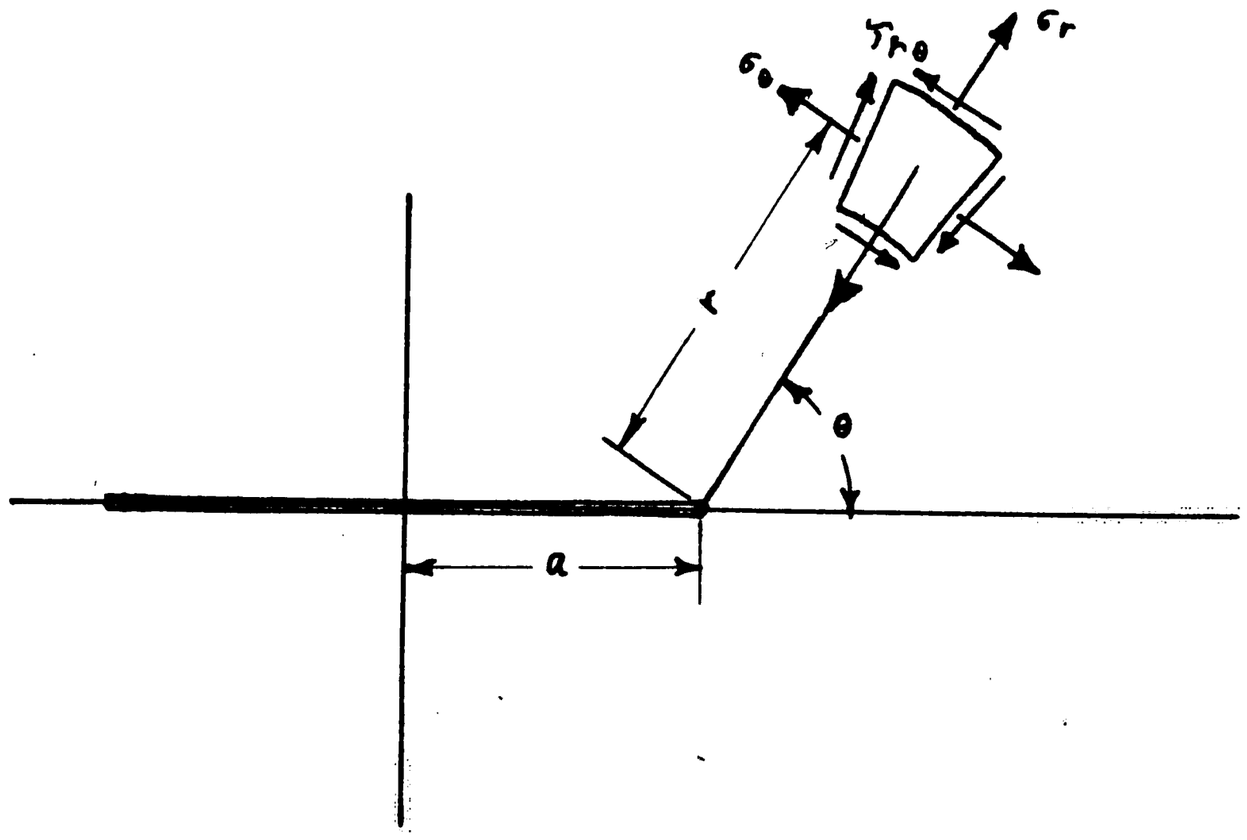

Figure 3

Coordinates of the Crack Tip

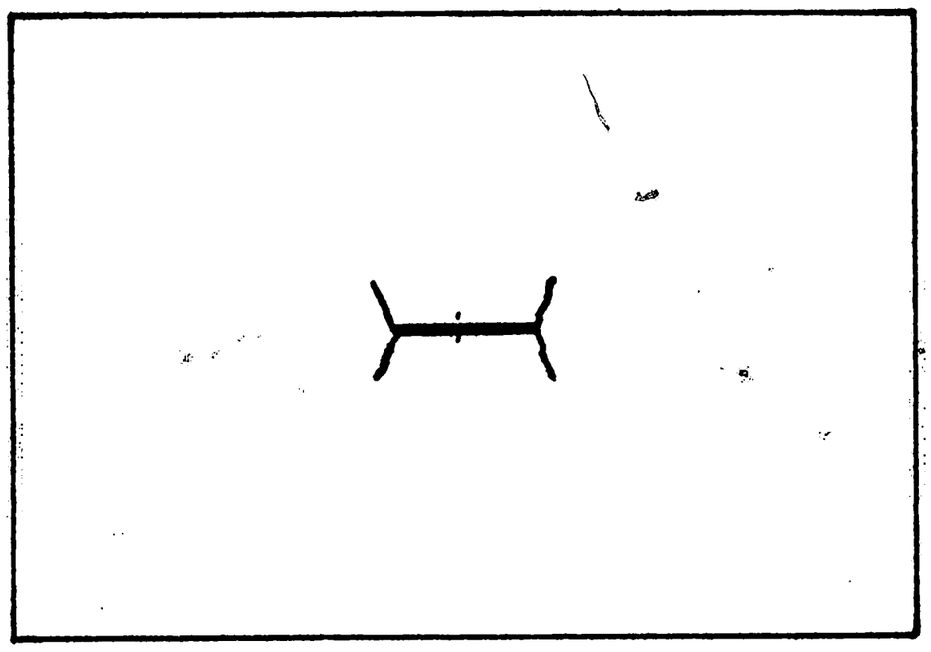

Figure 4

Crack Growth Under the Influence of the Transverse Shear Load Alone

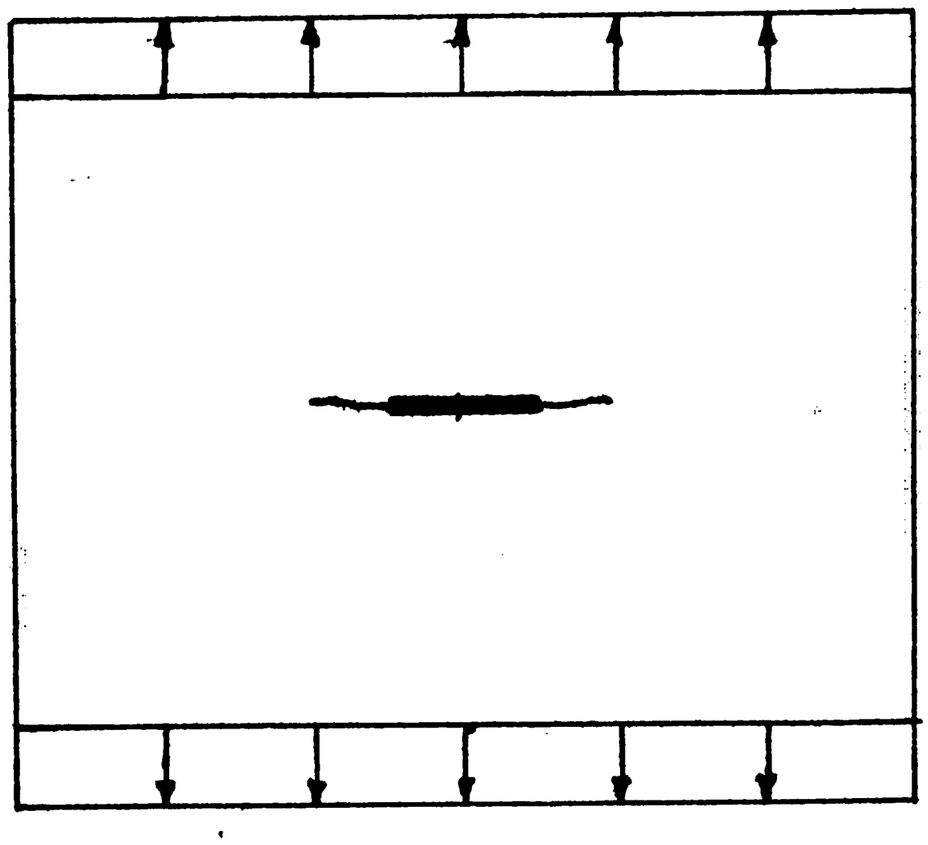

Figure 5

Crack Growth Under the Influence of Combined Tensile and Shear Loads

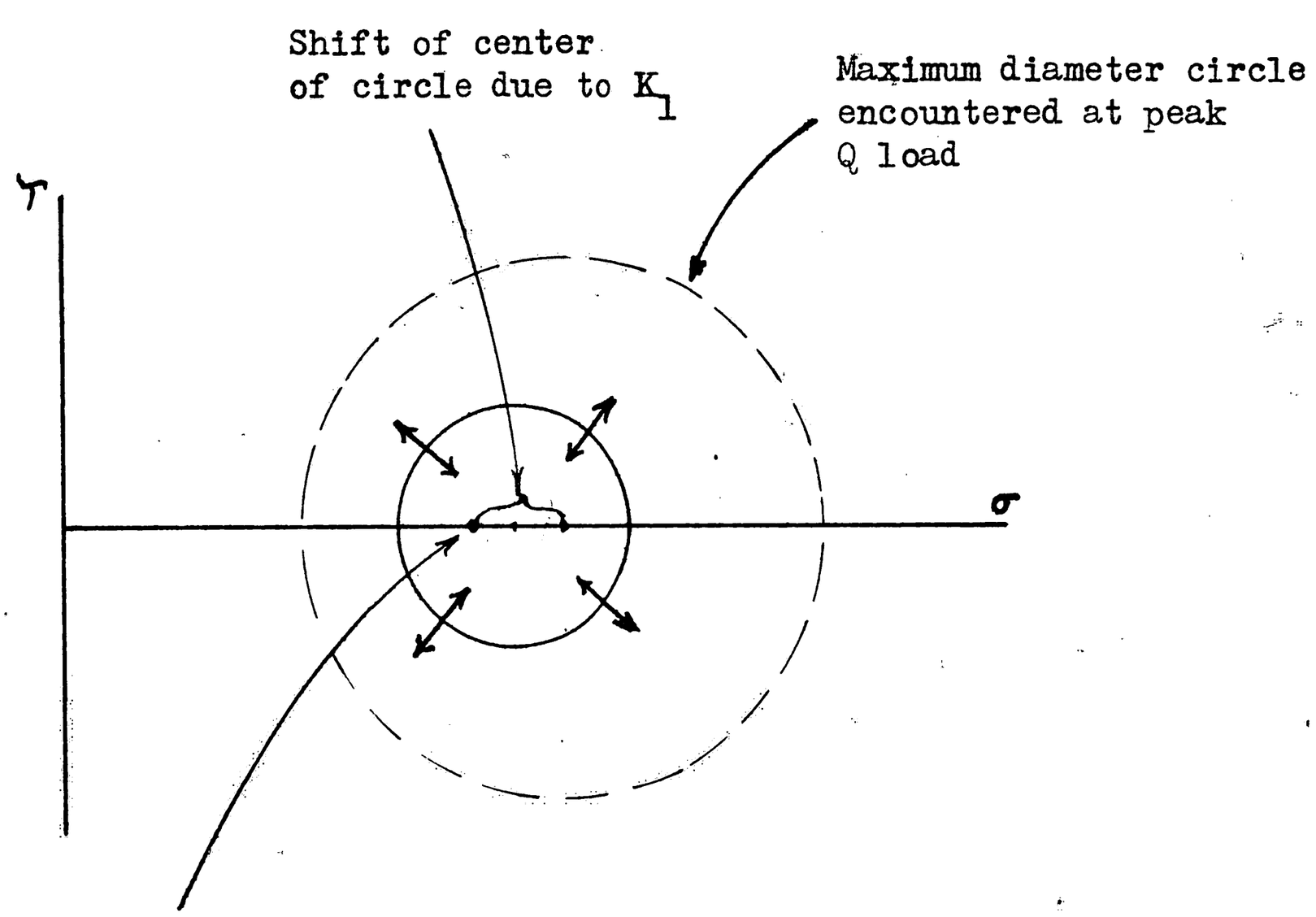

Figure 6

The Mohr Circle for Stress Near

the Crack Tip

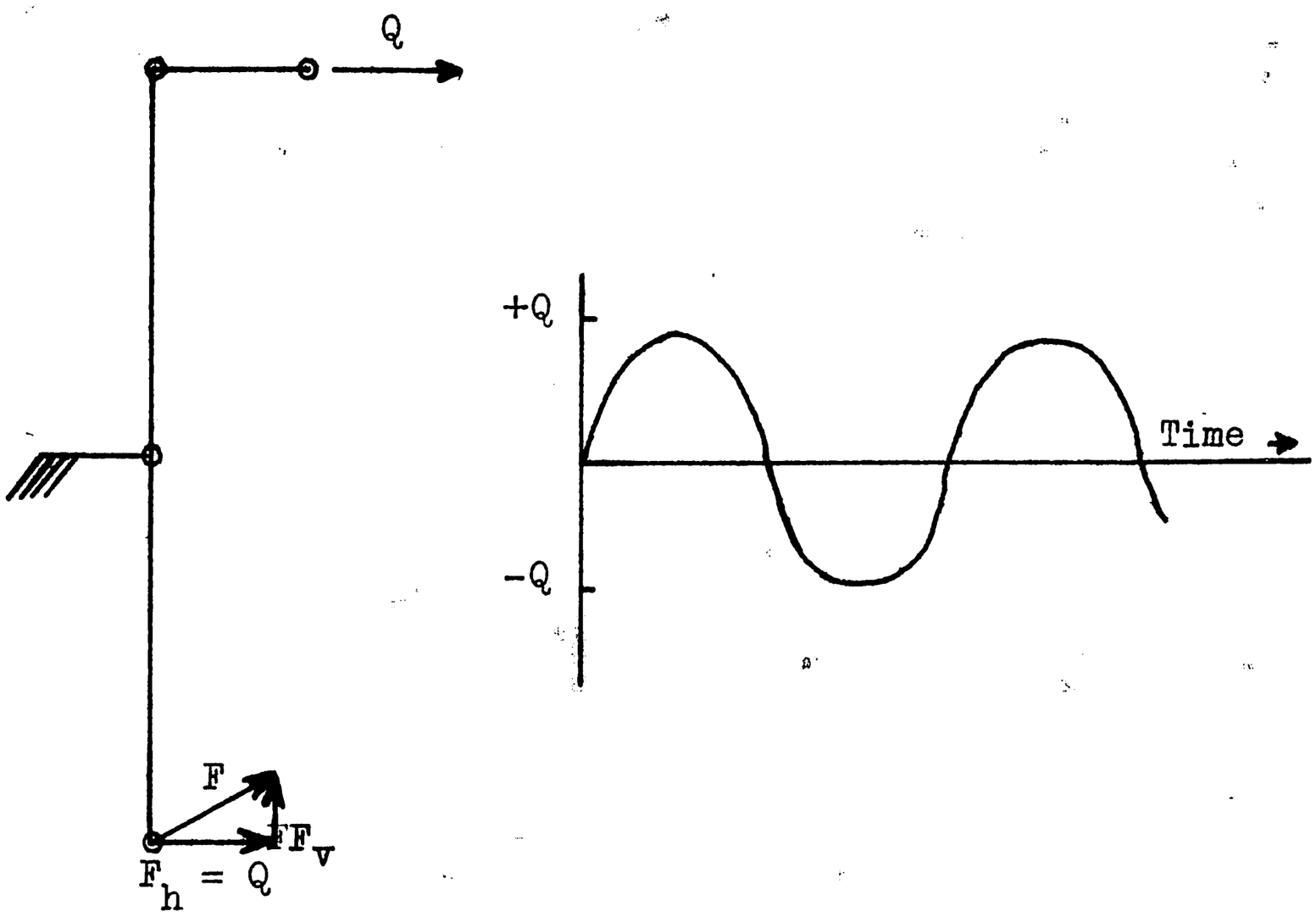

Figure 7

The Eccentric Loading Mechanism and the Plot of Its Horizontal Force Component

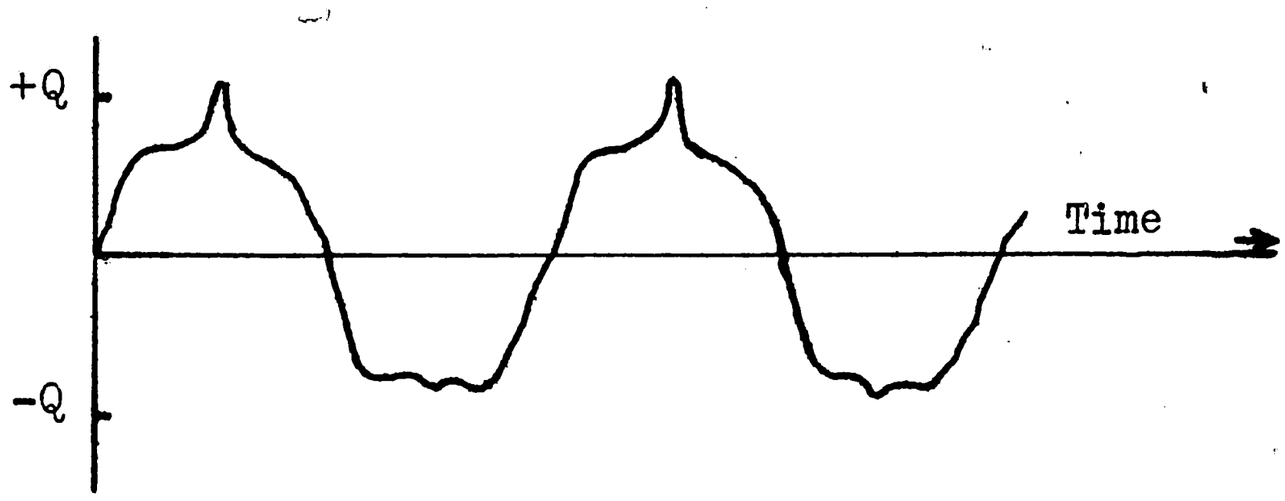

Figure 8

A Typical Load Vs. Time Variation Obtained With Torrington Needle Bearings

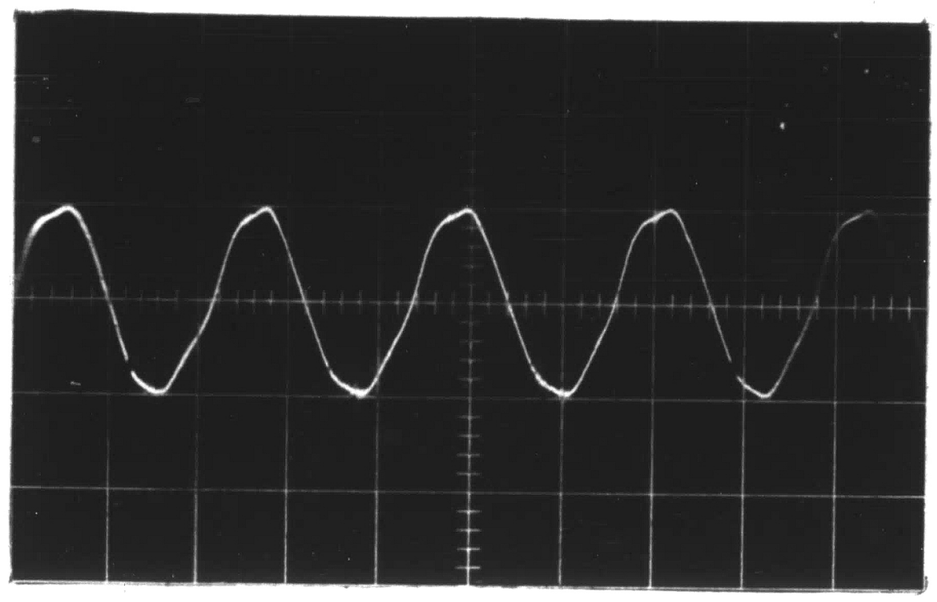

Figure 9

A Typical Load Time Variation Obtained With the Present Design

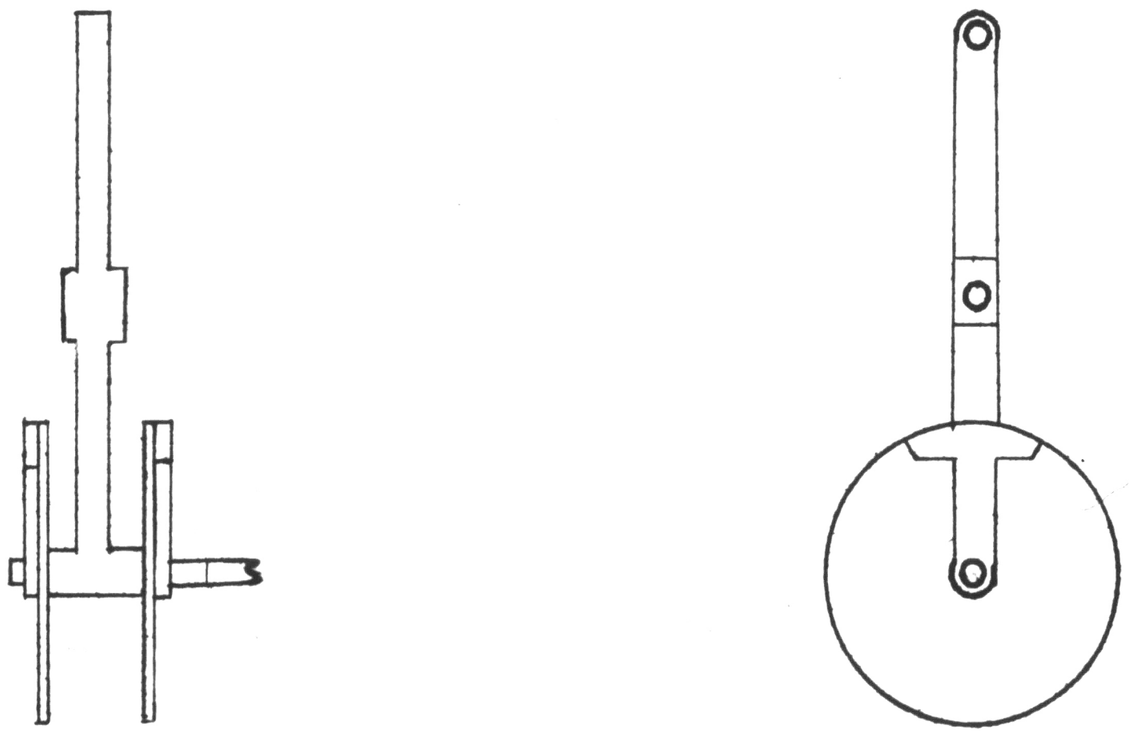

Figure 10

Two Views of the Loading Mechanism

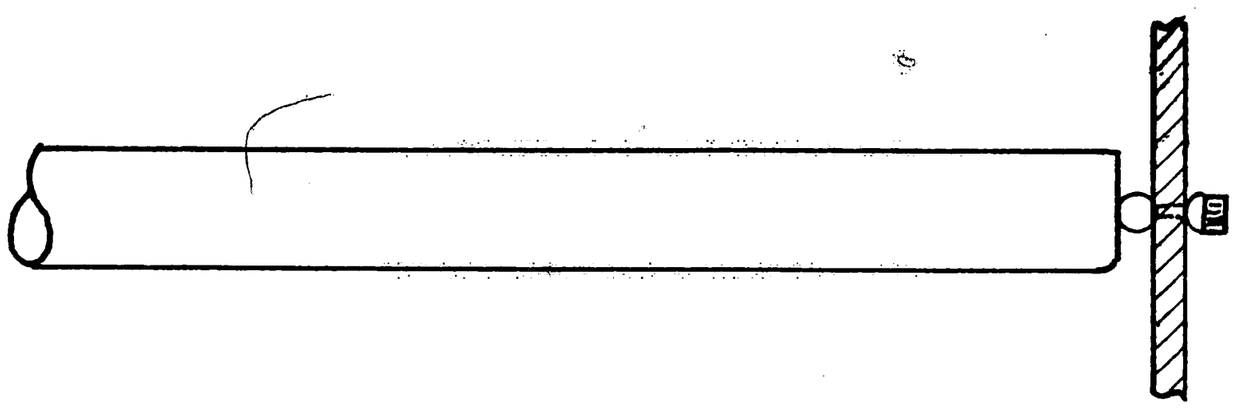

Figure 11

The Original Design of the Pin Connection to the Plate

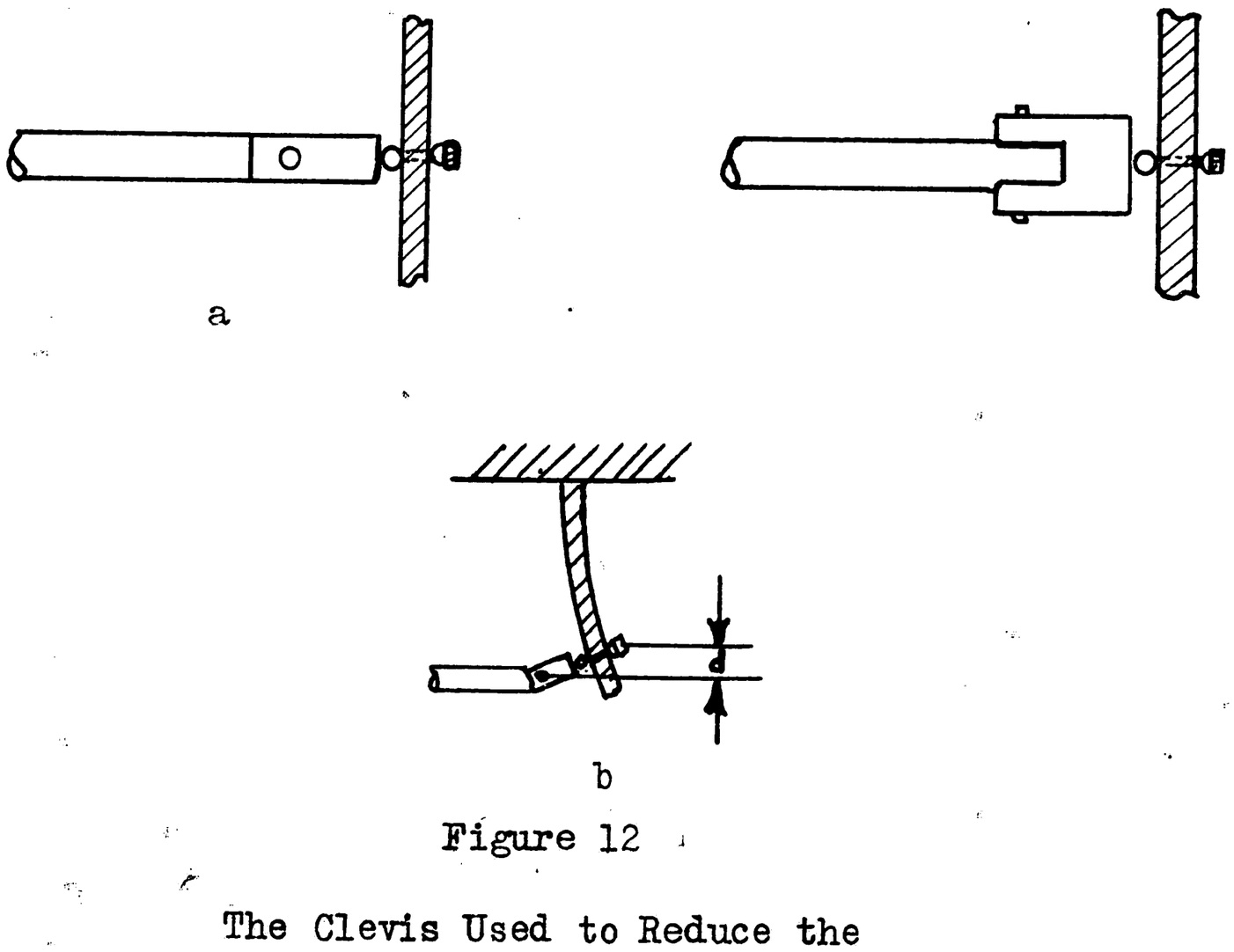

Figure 12

The Clevis Used to Reduce the

Moment Transmitted to the Plate

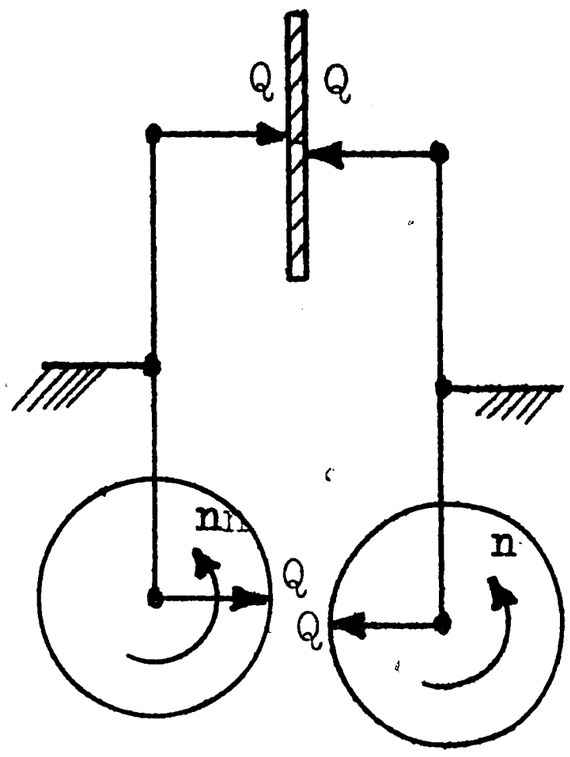

Figure 13

Two Eccentrics to Provide the Symmetric Loading

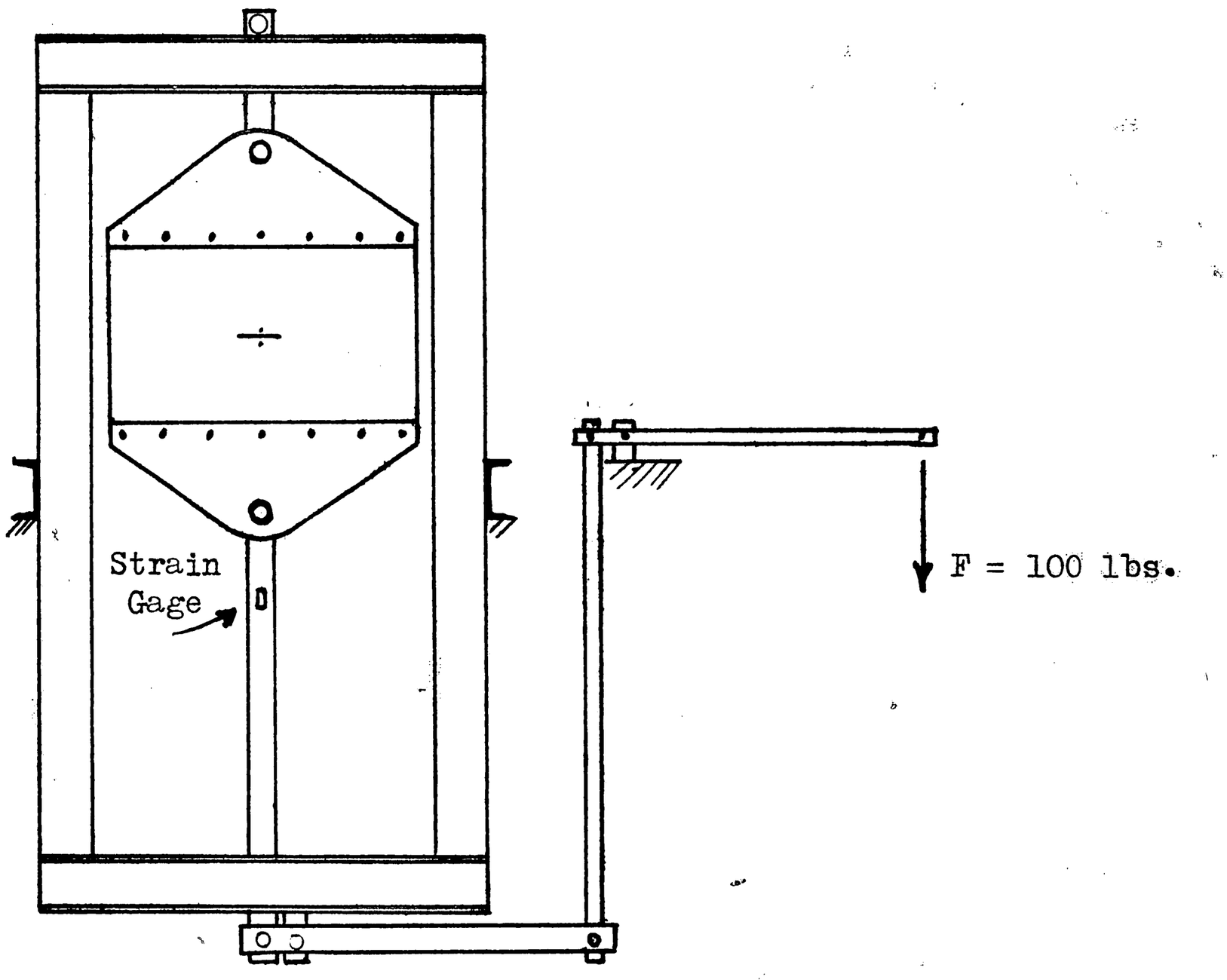

Figure 14

The Tensile Loading System

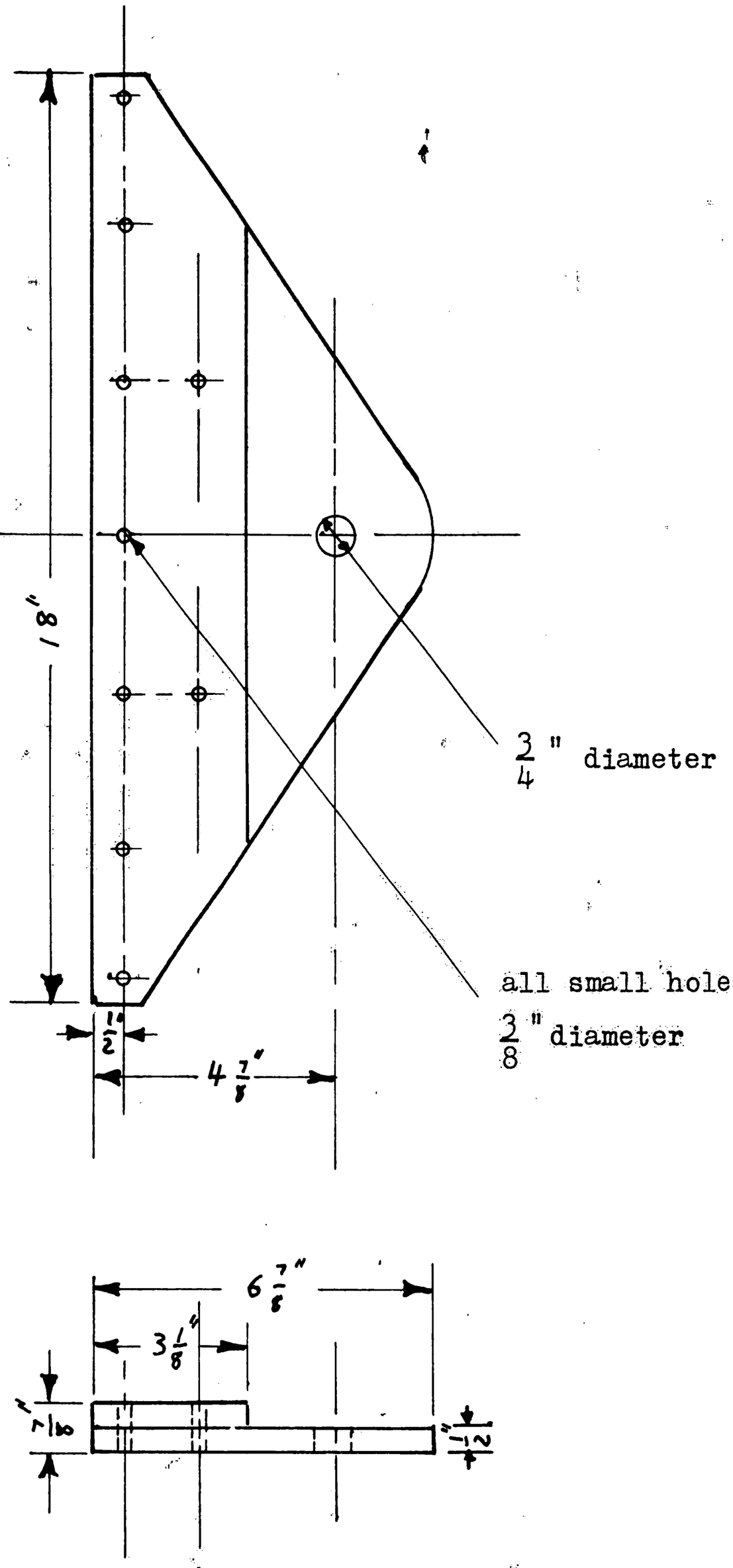

Figure 15

The Dimensions of the Jaw

Figure 16

Various Photographs of the Machine

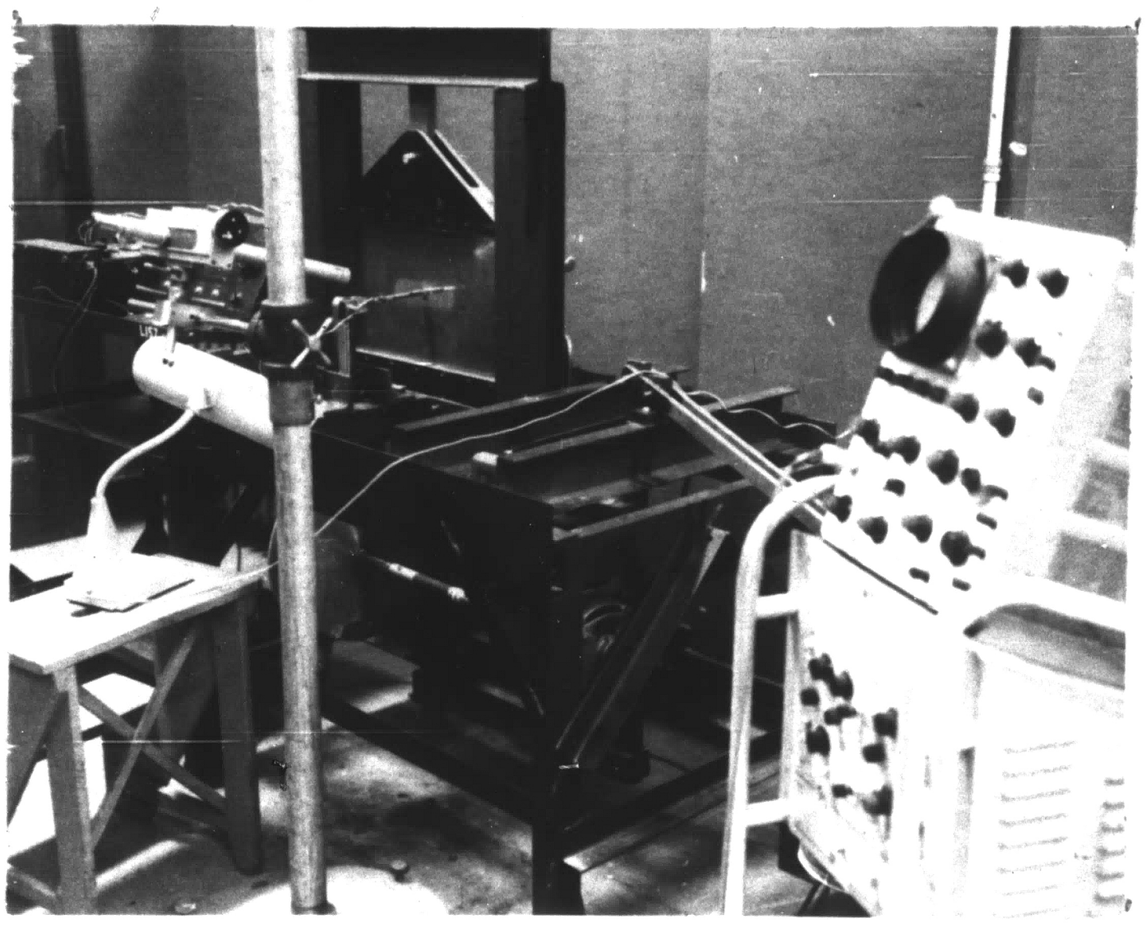

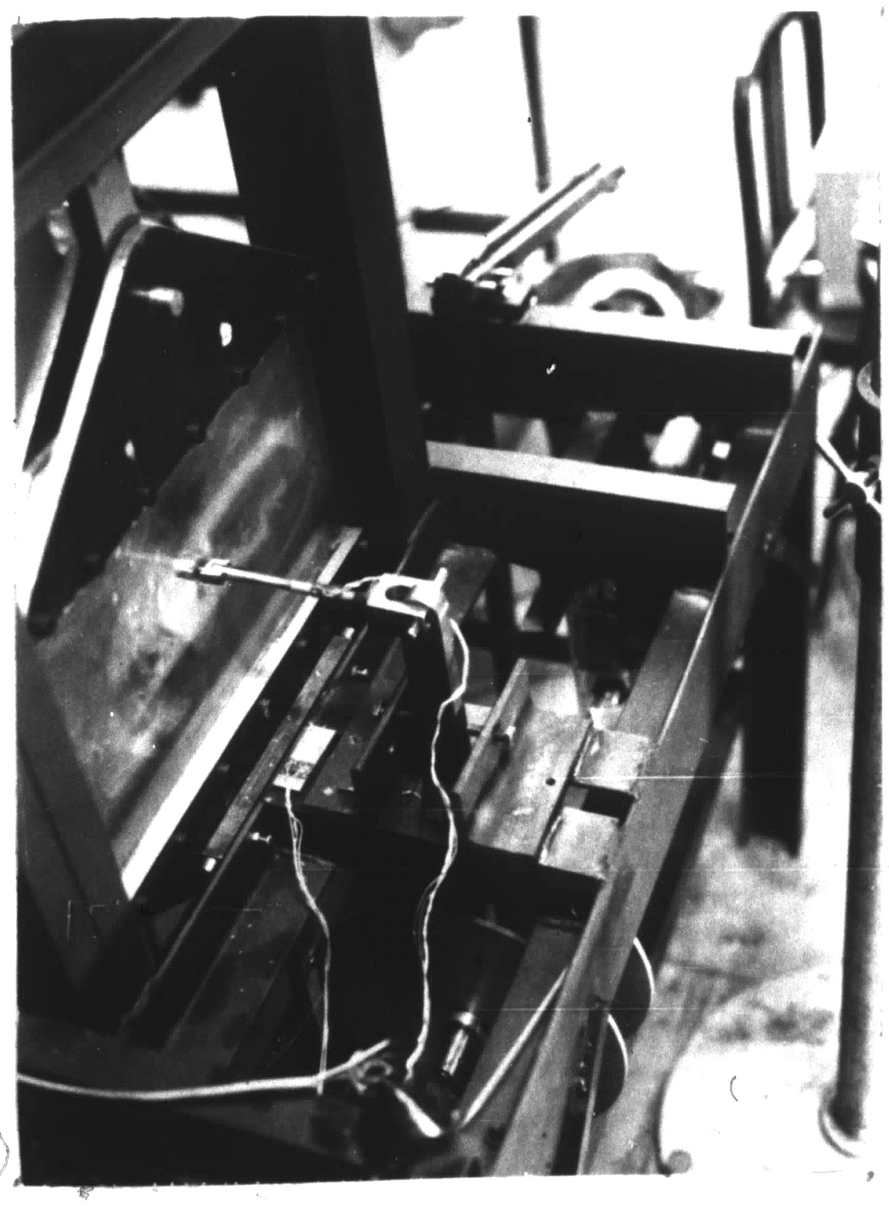

Figure 16 cont.

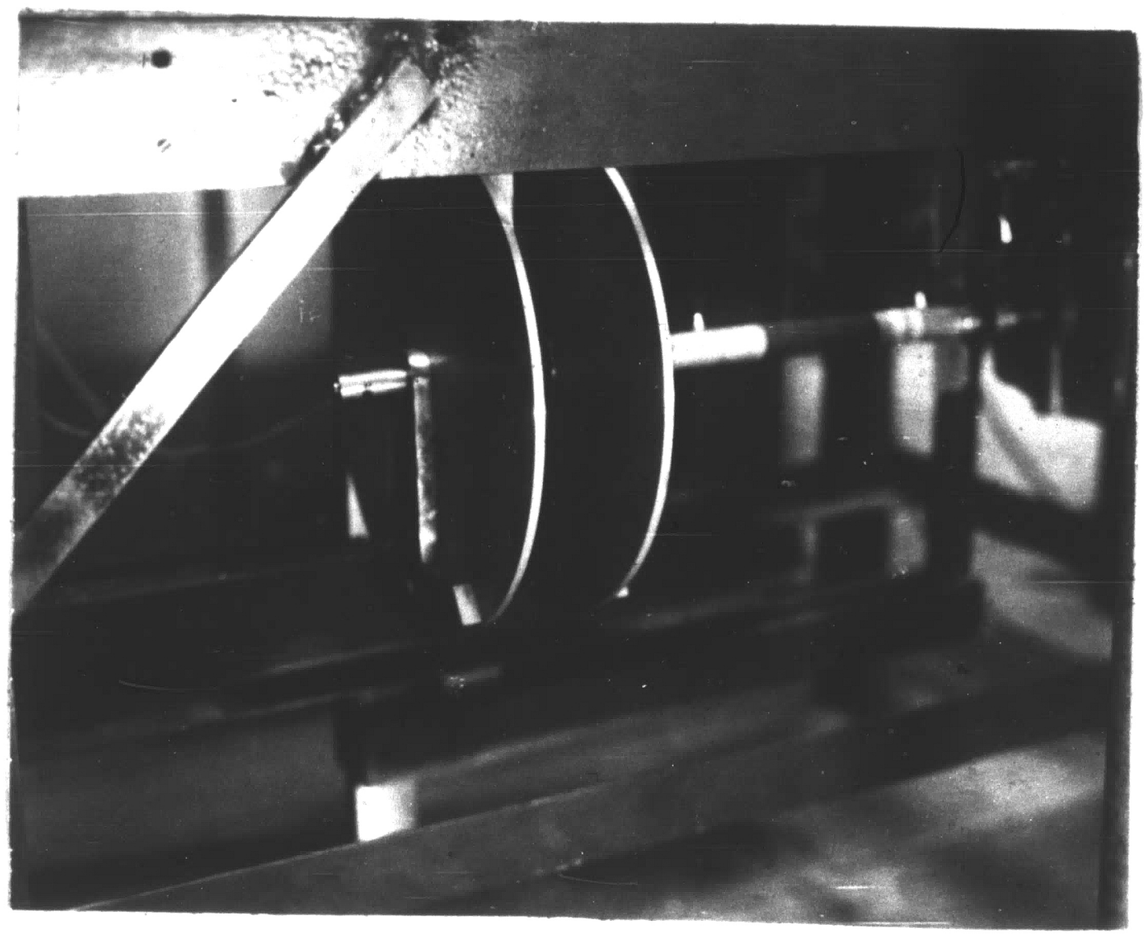

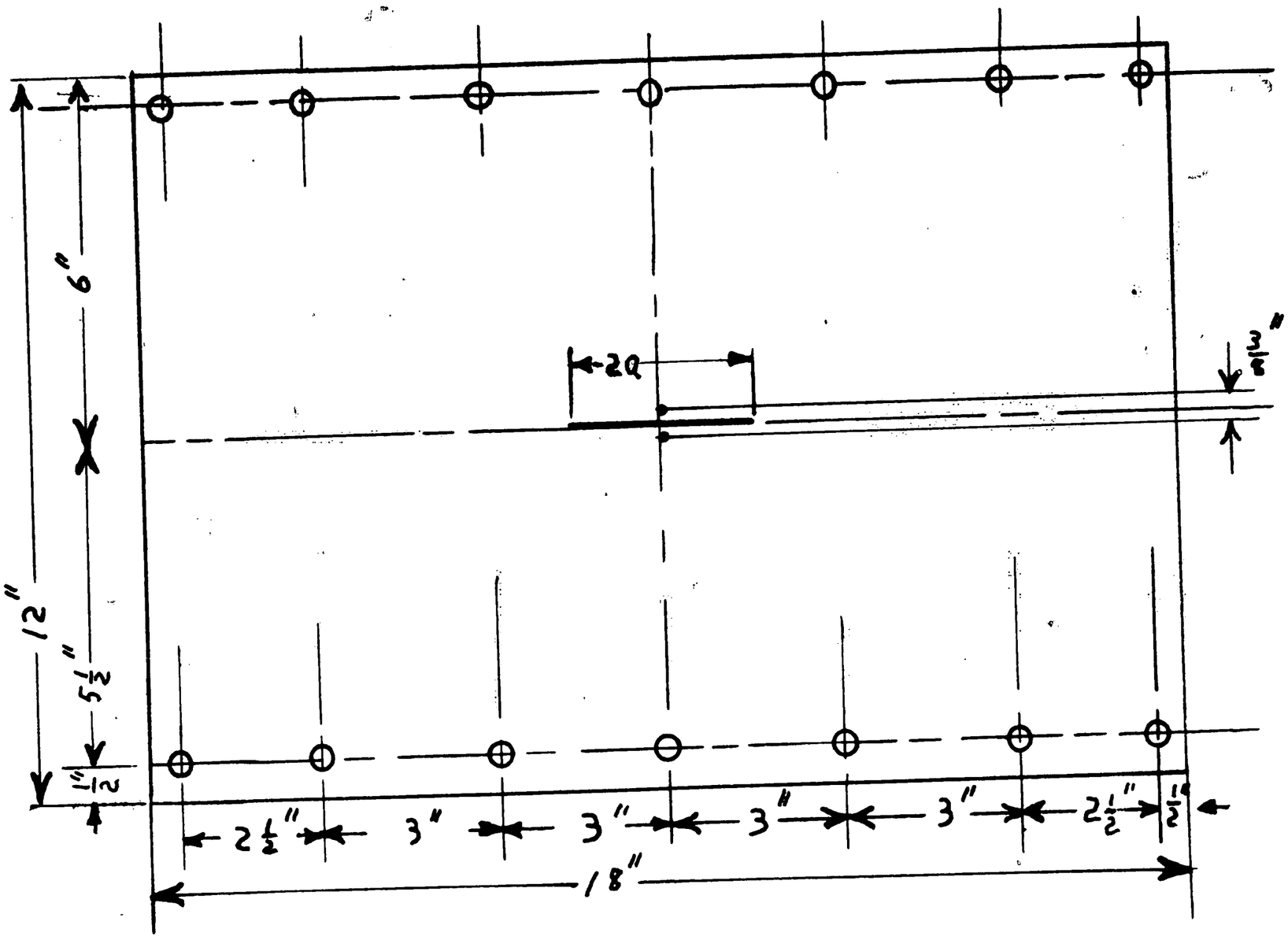

Figure 17

The Dimensions of the Test Specimen

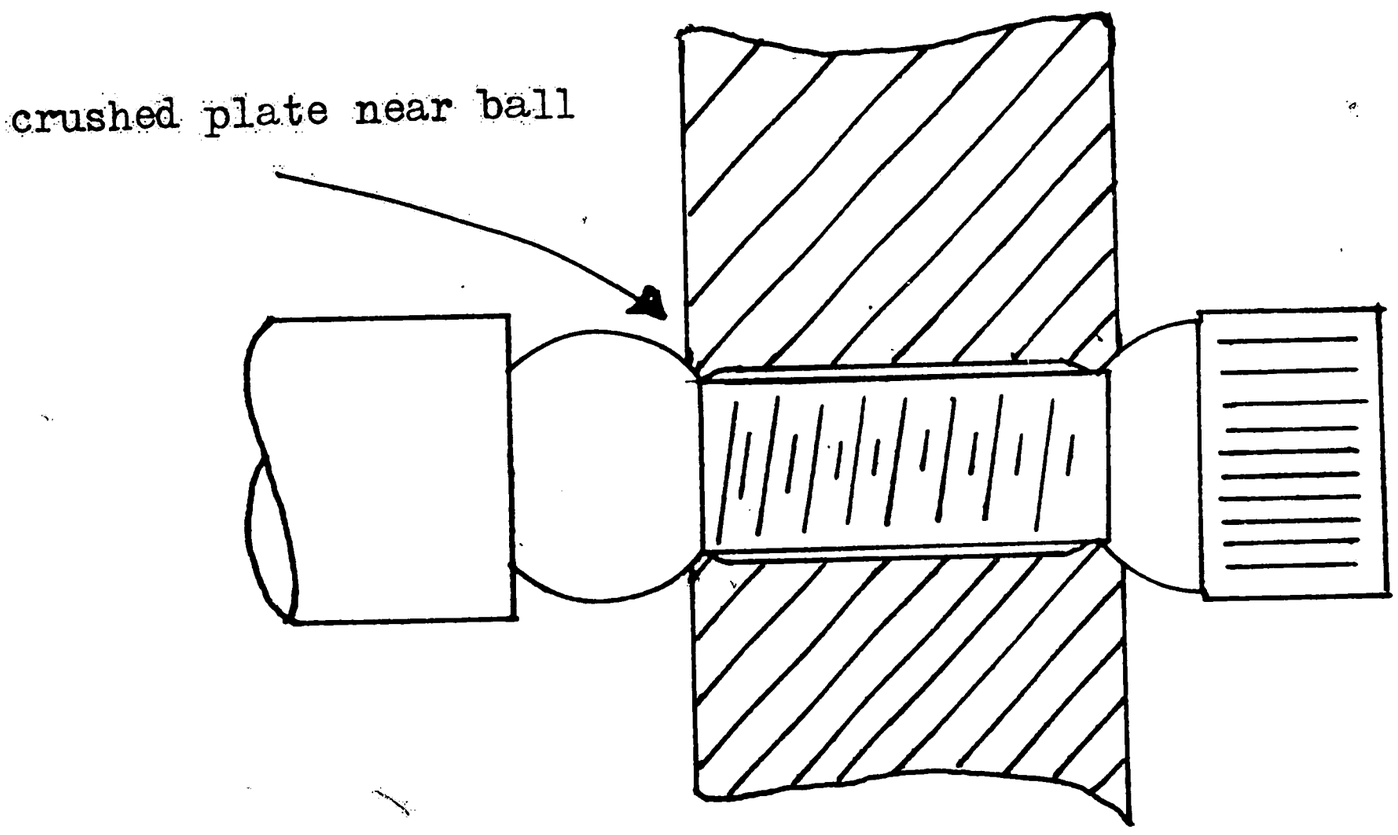

Figure 18

The Effect of an Extremely Tight Cap Screw

Figure 19

Plate I 2024-T3 Bare

h = 0.100 in.

Q = 157 lb.

Tensile Load 10,000 lbs.

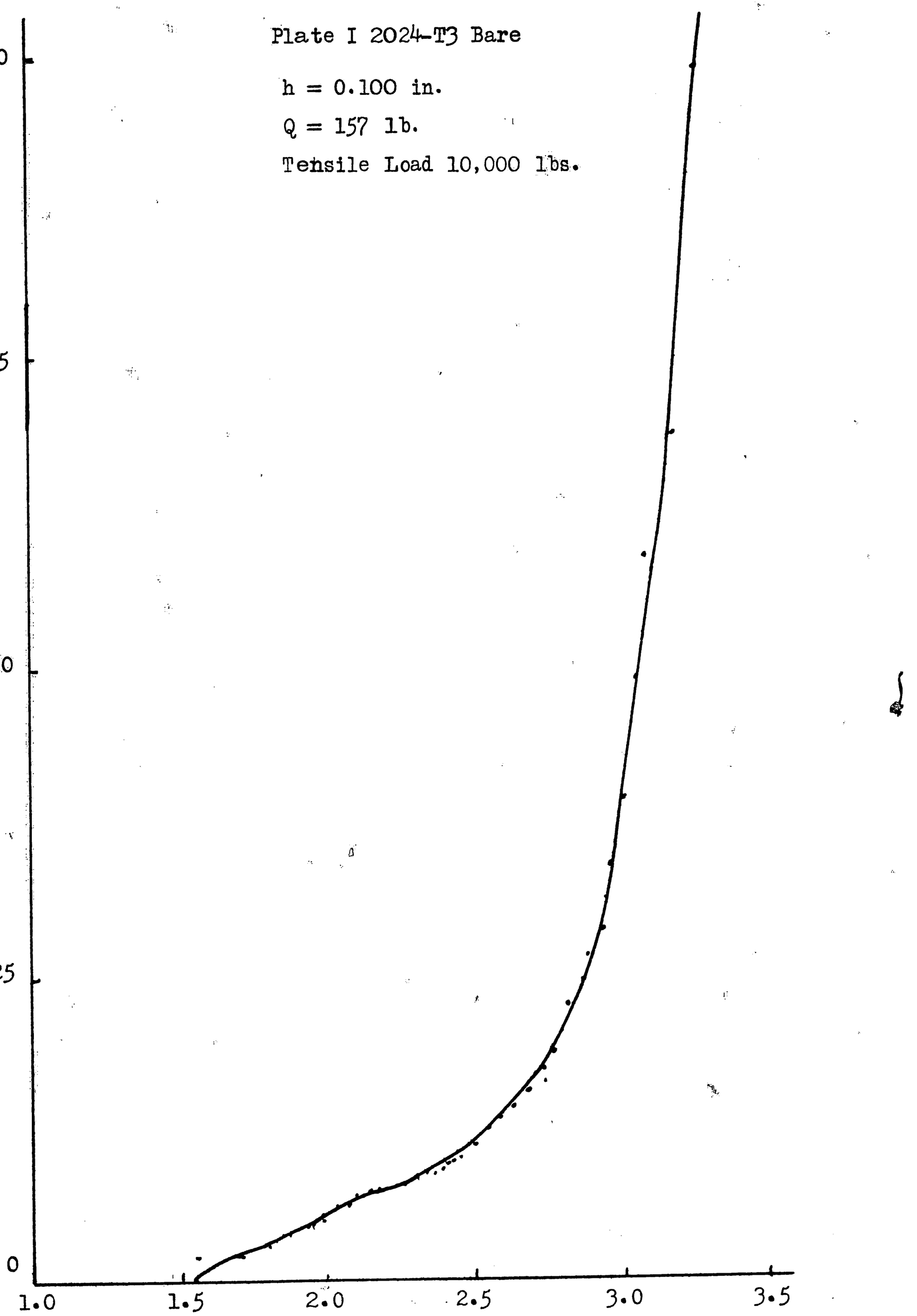

Figure 20

Crack Length VS. No. of Cycles Curve

Plate II

2024-T3 Bare

h = 0.100 in.

Q = 157 lb.

Tensile Load 10,000 lbs.

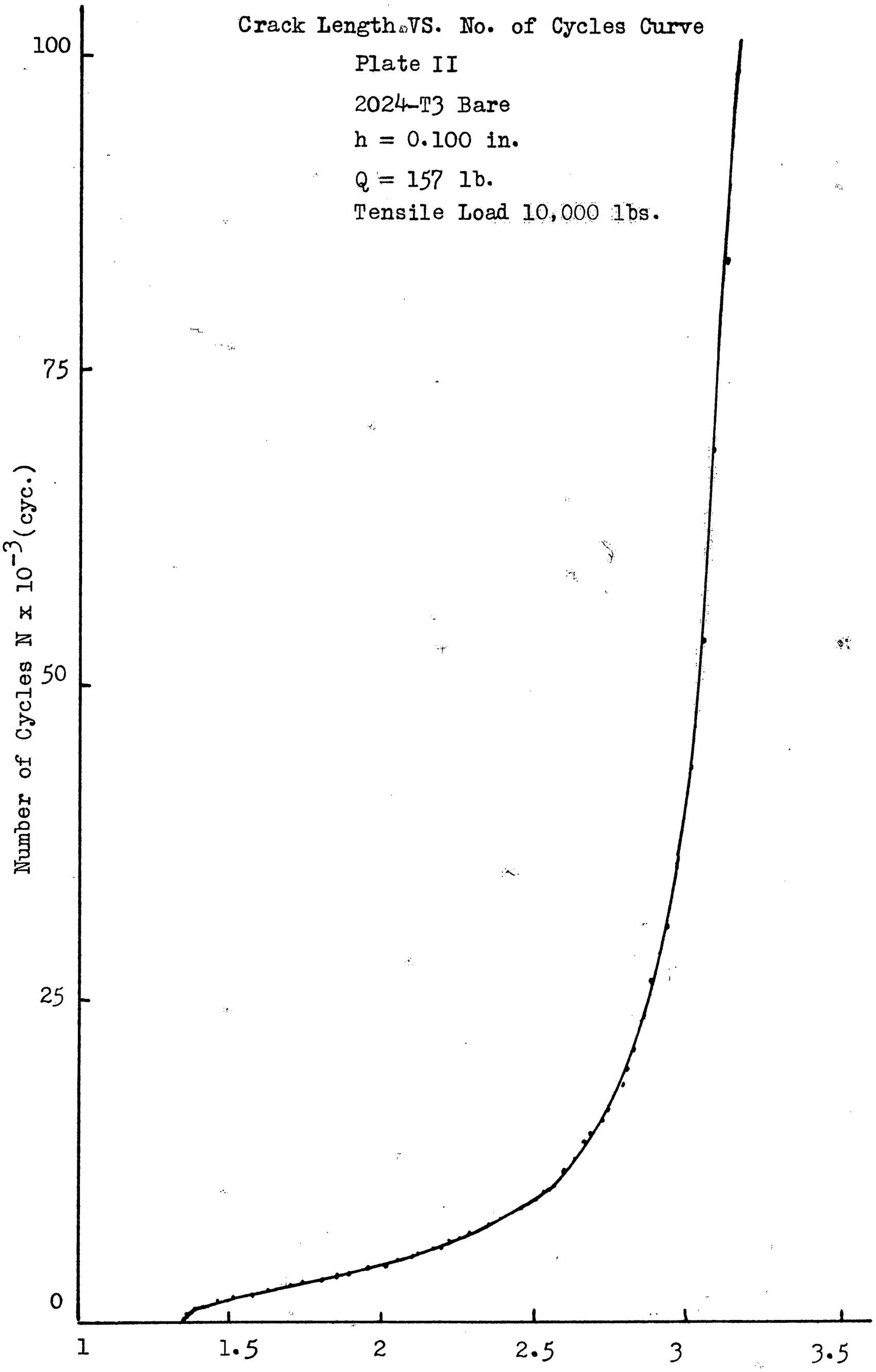

Figure 21

Crack Length Vs. No. of Cycles Curve

Plate III 2024-T3 Bare

h = 0.100 in.

Q = 157 lb.

Tensile Load 10,000 lbs.

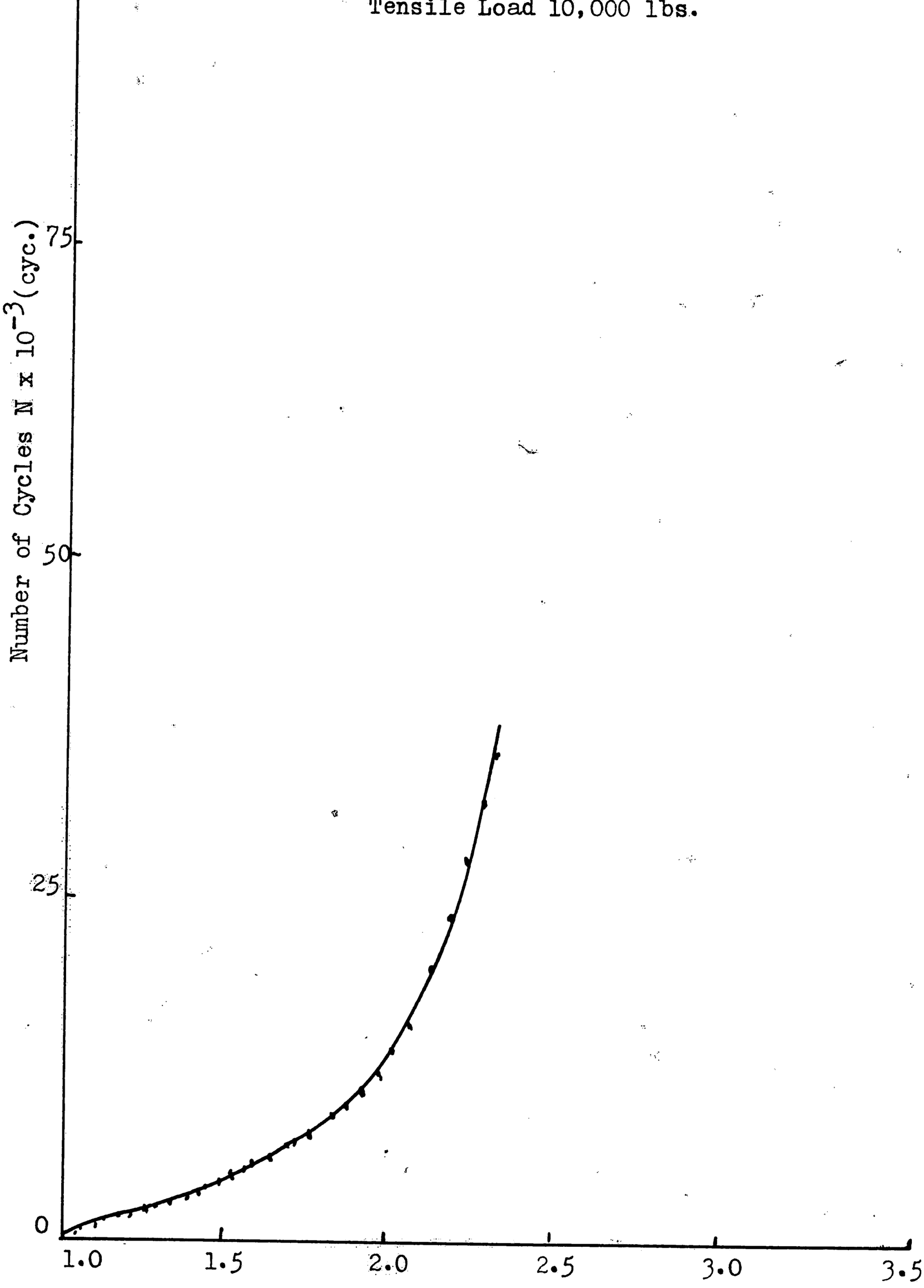

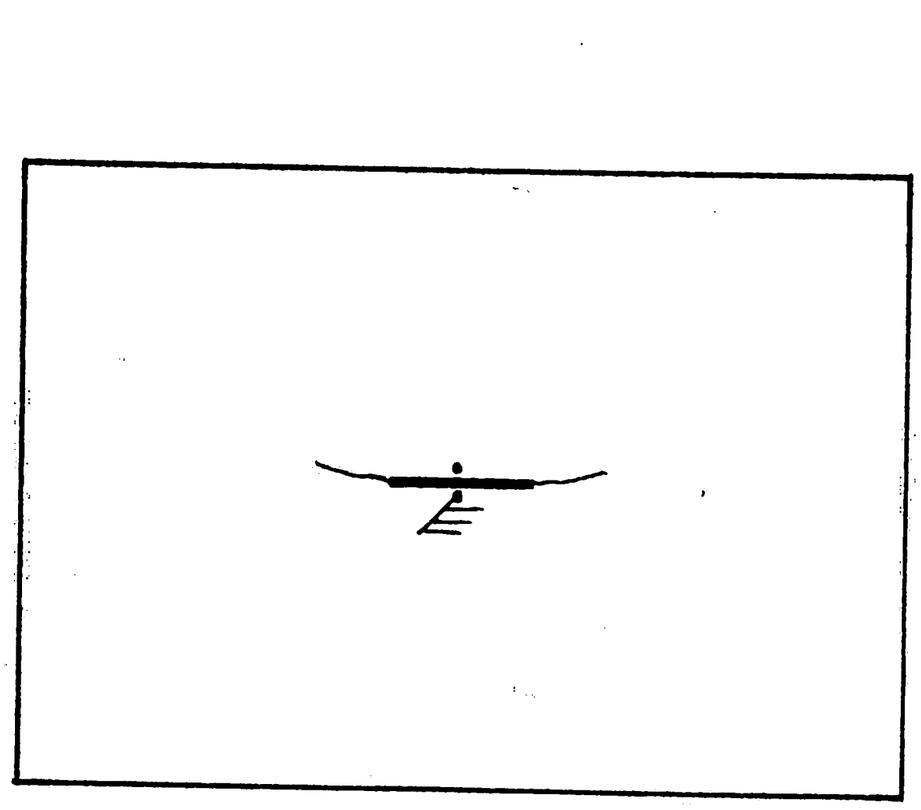

Figure 22

The Direction of Crack Growth When One Crack Edge is Fixed

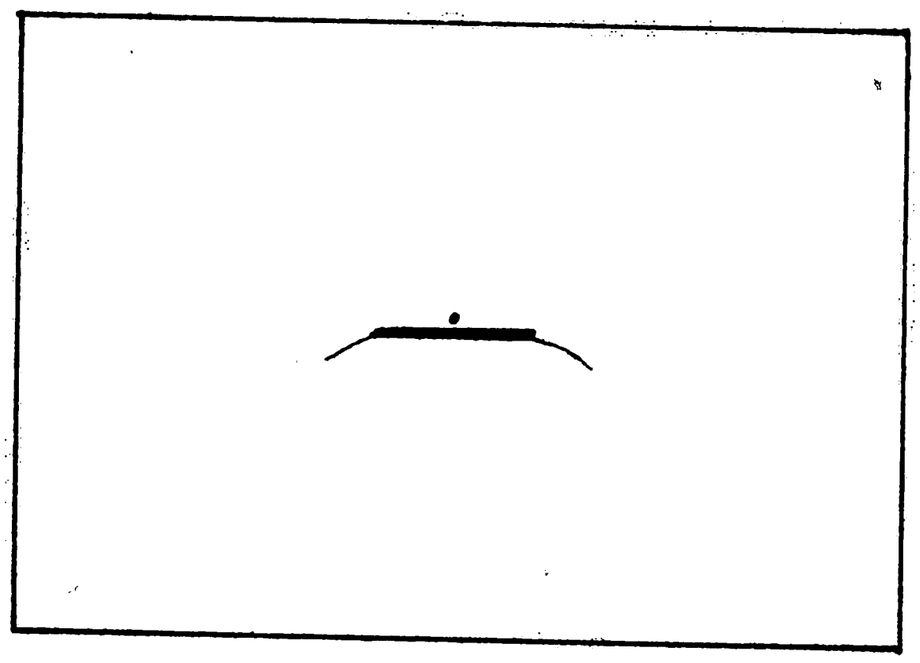

Figure 23

The Direction of Crack Growth When One Crack Edge Is Free

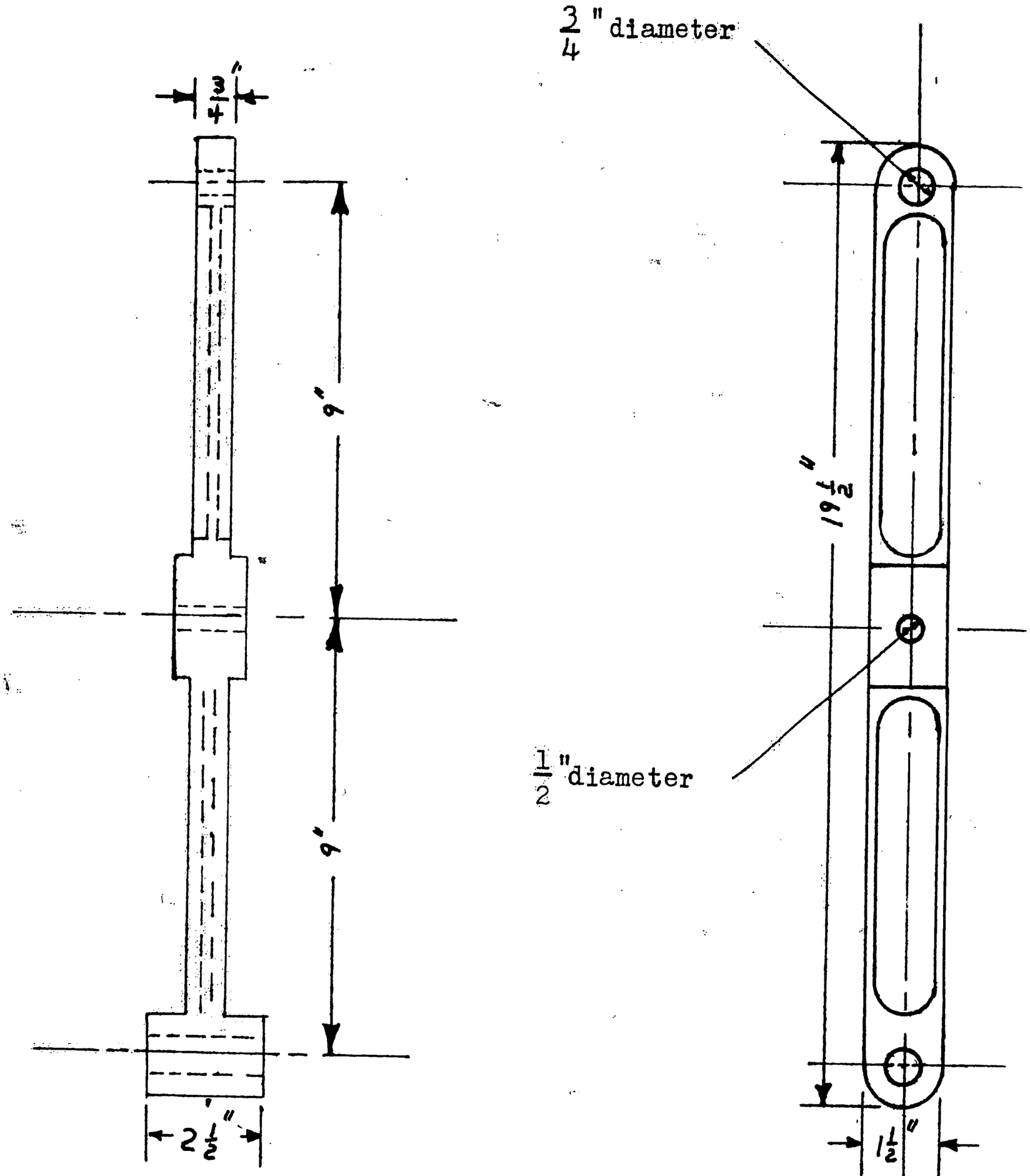

Figure 24

Dimensions of the Pivot Arm

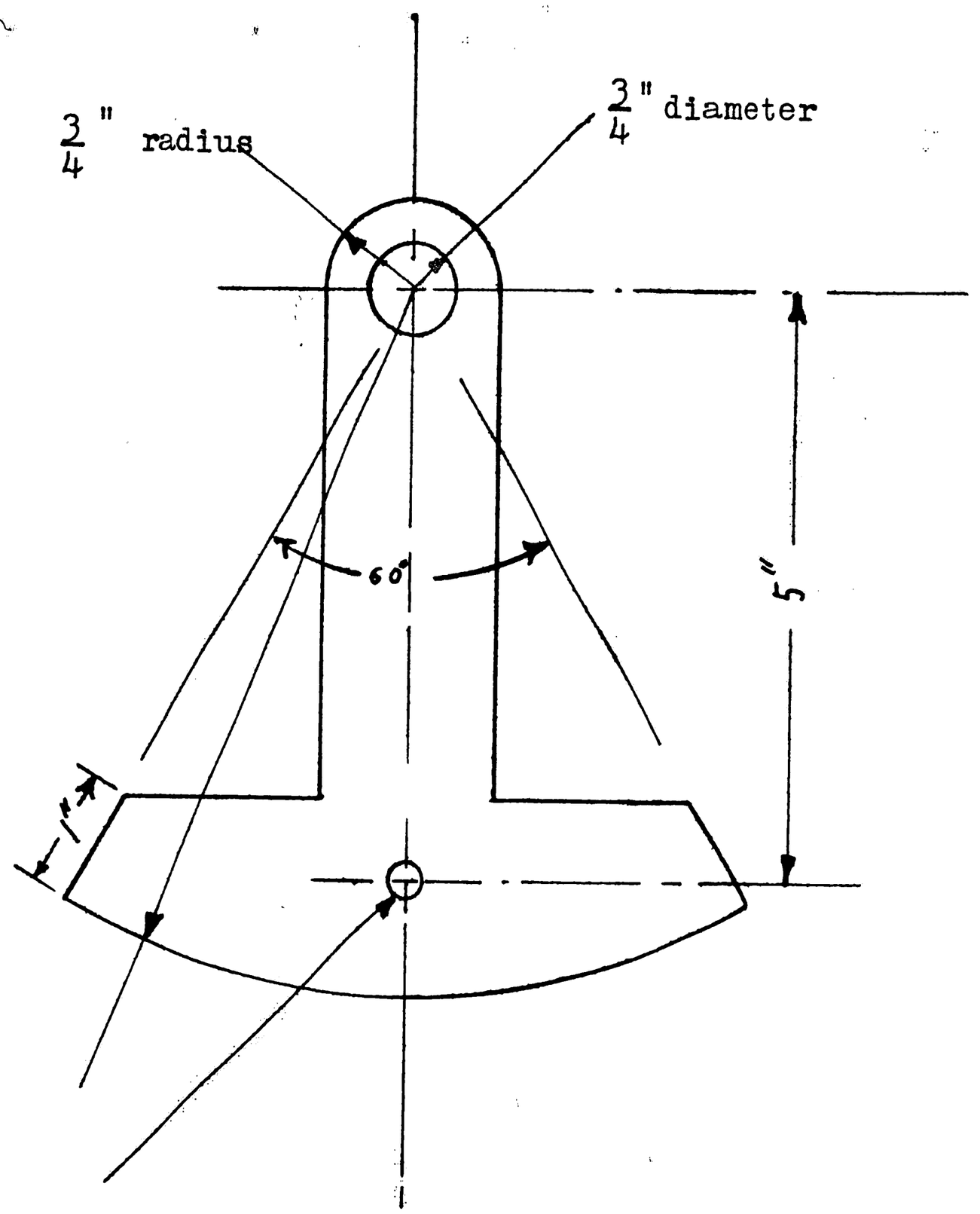

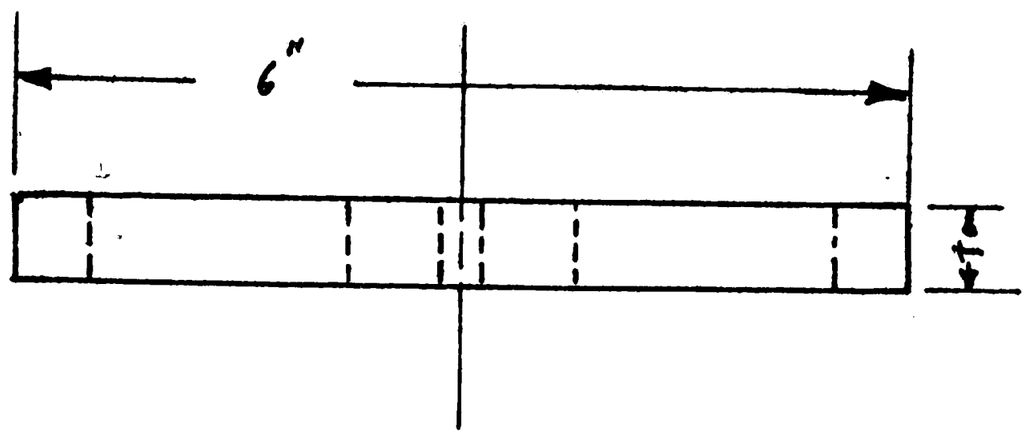

Figure 25

Dimensions of the Eccentric

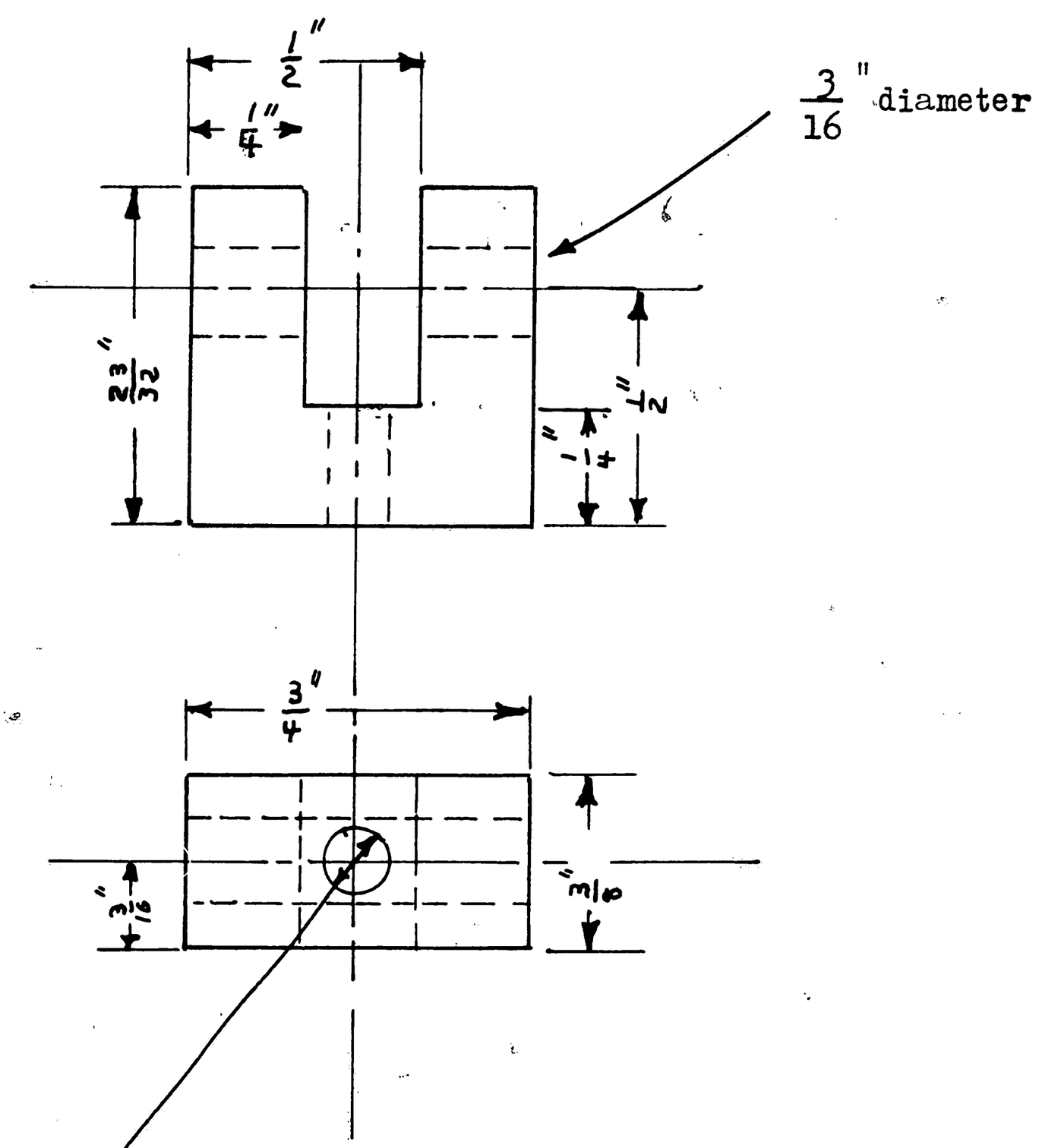

Figure 26

Dimensions of the Clevis

Figure 27

Load Speed Curve for an Uncracked Plate

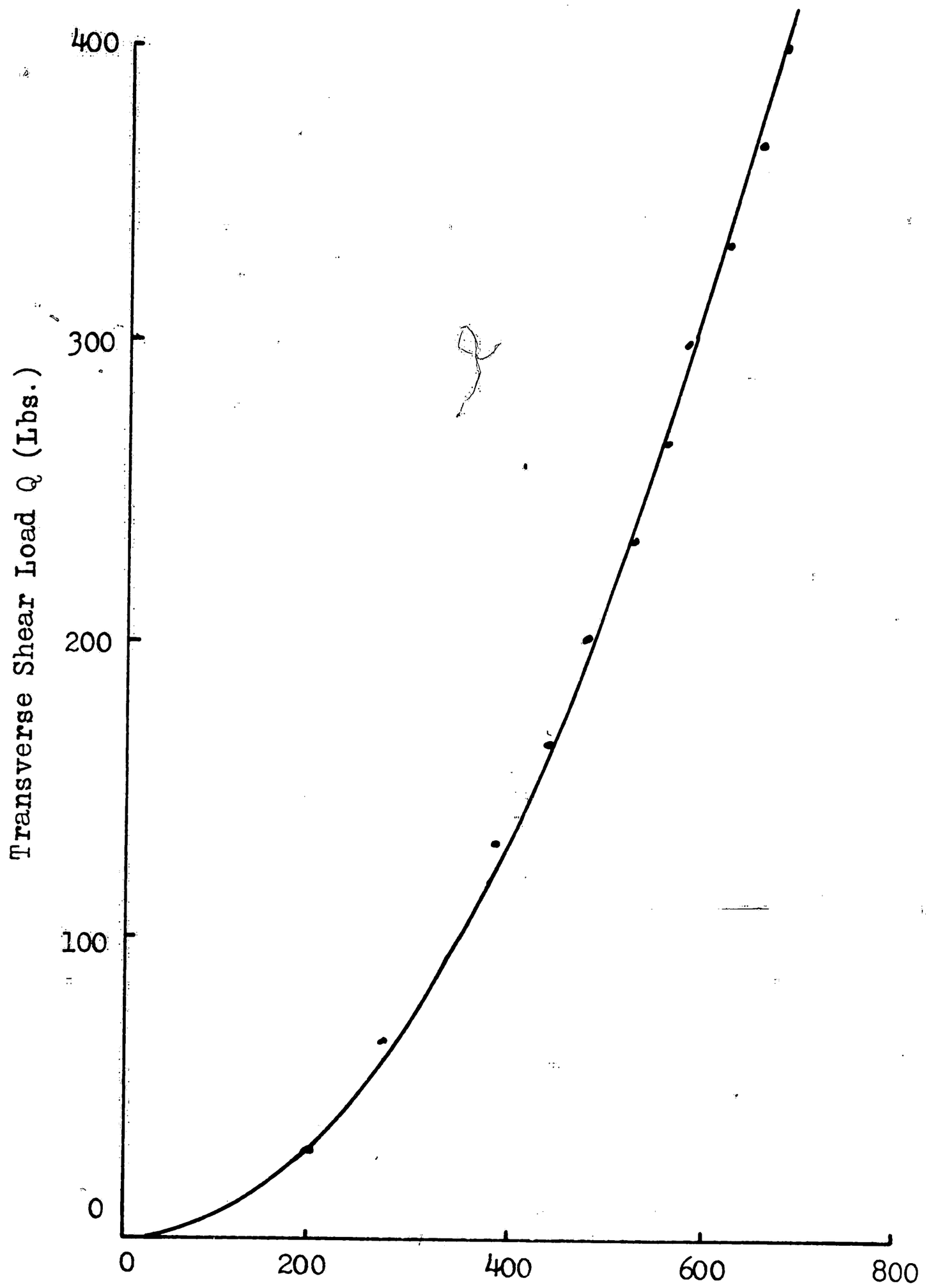

Figure 28

Eccentric Speed VS. Crack Length Curve

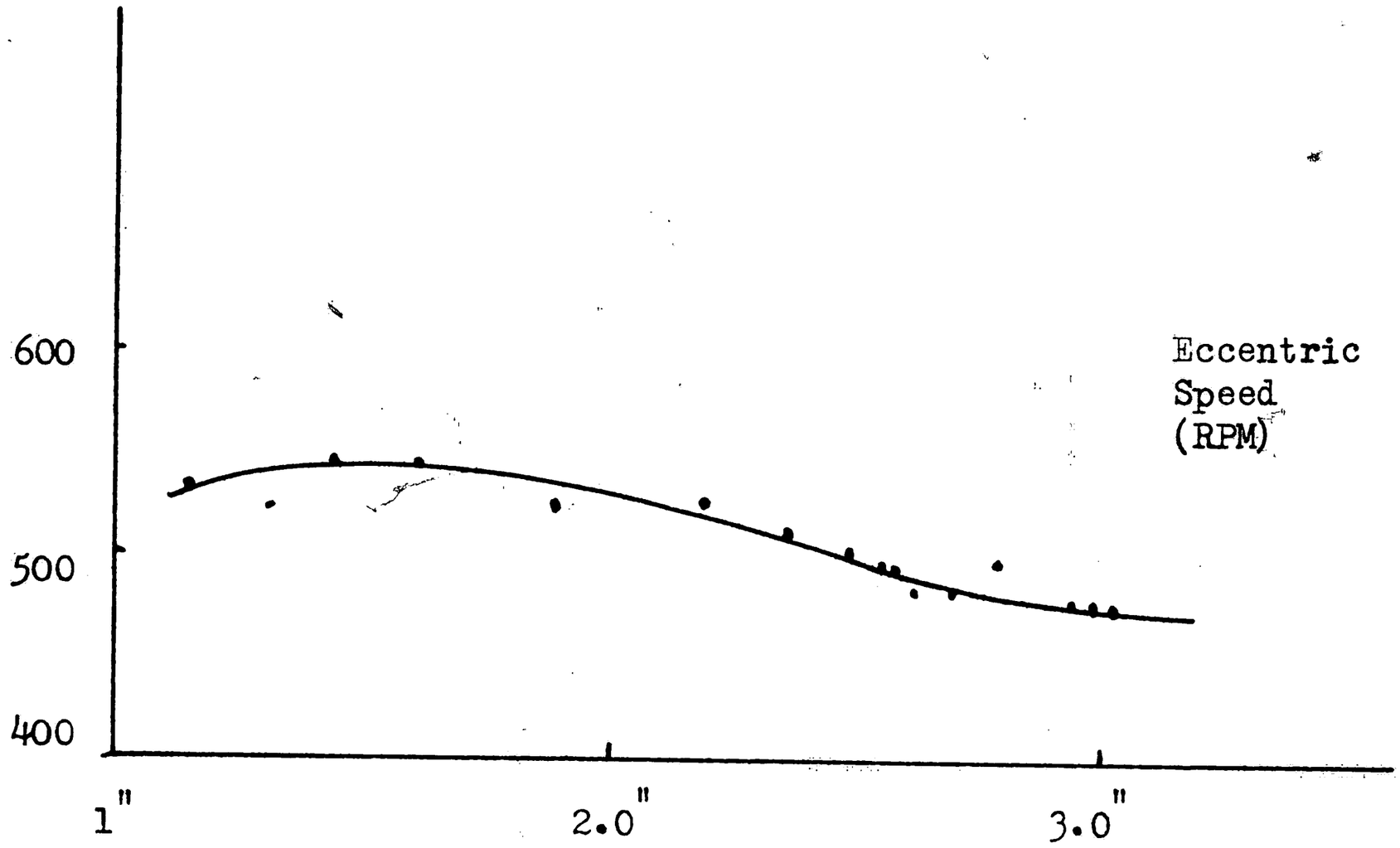

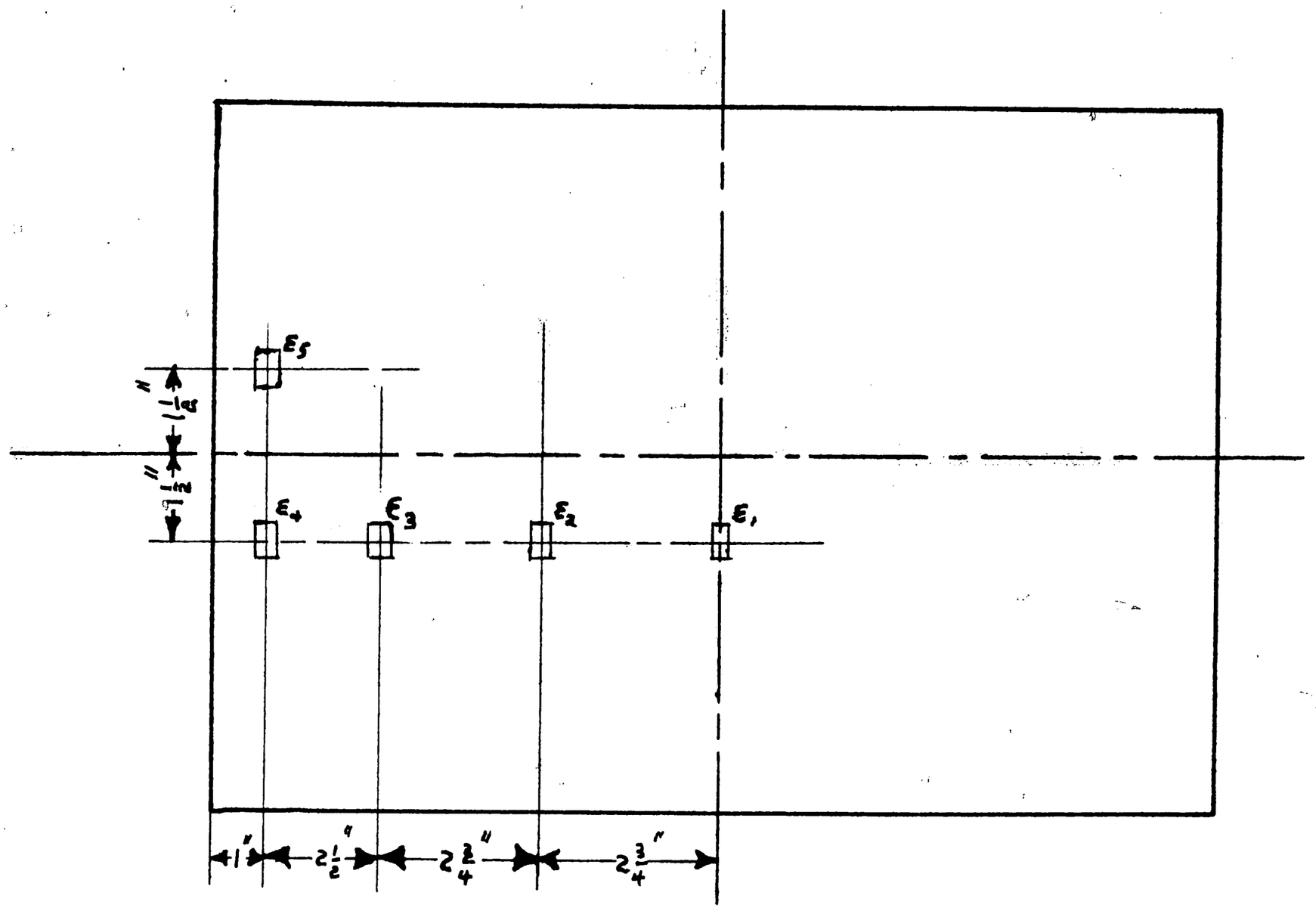

Figure 29

The Placement of the Strain Gages

References

1. Paris, P., "The Growth of Cracks Due to Variations in Load", Ph.D. Dissertation, Lehigh University, 1962.

2. Erdogan, F. and Roberts, R., "A Comparative Study of Crack Propagation in Plates Under Extension and Bending", a Progress Report Prepared for the NASA, Lehigh University, March 1965.

3. Roberts, R., "On the Rate of Crack Propagation Due to Fluctuating Bending Loads", Ph.D. Dissertation, Lehigh University, 1964.

4. Erdogan, F.and Sih, G.C., "On Crack Extension in Plates Under Plane Loading and Transverse Shear", Institute of Research Report, Lehigh University, June 1962.

5. Erdogan, F. and Feridum, K.K., private communication, June 1964.

6. Erdogan, F., Paris, P. and Sih, G., "Crack Tip Intensity Factors for Plane Extension and Plane Bending Problems", Journal of Applied Mechanics Transactions, ASME, Paper No. 61-APMW-29.

7. Schijve, J., "Analysis of the Fatigue Phenomenon in Aluminum Alloys", National Aero and Astronautical Research Institute, Amsterdam, TRM. 2122, April 1964.

8. Dugdale, D.S., "Yielding of Steel Sheets Containing Slits", Jour. Mech. Phys. Solids, vol. 8, p. 100, 1960.

Vita

William James Valentine was born in New York City on January 2, 1942, to Donald and Martha Valentine. He received his secondary education in the Ridgewood New Jersey school system. He did both his undergraduate and graduate studies in the Department of Mechanical Engineering of Lehigh University. During his undergraduate career he was elected to Pi Tau Sigma and Tau Beta Pi. He was also a recipient of the William Gotshall Scholarship for the 1964-65 academic year.